UNIVERSITY OF SOUTHAMPTON

INSTITUTE OF SOUND AND VIBRATION RESEARCH

FLUID DYNAMICS AND ACOUSTICS GROUP

The estimation of geoacoustic properties from broadband acoustic data, focusing on Instantaneous frequency techniques

by

G.B.N. Robb, P.R. White, J.M. Bull, A.I. Best, T.G. Leighton and J.K. Dix.

ISVR(technical report) No. 298

August, 2002

Authorised for issue by
Professor C L Morfey
Group Chairman

ACKNOWLEDGEMENTS

	Contents	Page

Acknowledments *ii*

LIST OF FIGURES AND TABLES.   **PAGES.**

Abstract

The compressional wave velocity and attenuation of marine sediments are fundamental
to marine science. In order to obtain reliable estimates of these parameters it is
necessary to examine in situ acoustic data, which is generally broadband. A variety of
techniques for estimating the compressional wave velocity and attenuation from
broadband acoustic data are reviewed. The application of Instantaneous Frequency (IF)
techniques to data collected from a normal-incidence chirp profiler is examined. For the
datasets examined the best estimates of IF are obtained by dividing the chirp profile into
a series of sections, estimating the IF of each trace in the section using the first moments
of the Wigner Ville distribution, and stacking the resulting IF to obtain a composite IF
for the section. As the datasets examined cover both gassy and saturated sediments, this
is likely to be the optimum technique for chirp datsets collected from all sediment
environments.

LIST OF ABBREVIATIONS.

BT product: Bandwidth-Duration product.

DCTF: Discrete classical time formulae.

IF: Instantaneous Frequency.

LSR: Log-spectral-ratio.

PWVD: Polynominal Wigner-Ville distribution.

SNR: Signal to noise ratio.

STFT: Short time Fourier transform.

TFD: Time-frequency distribution.

WVD: Wigner-Ville distribution.

XWVD: Cross Wigner-Ville distribution.

List of symbols

x	Distance traveled by an acoustic wave	(m)
t	Time over which acoustic pulse has traveled (ms)	
A_o	Amplitude of acoustic pulse at $t = 0$ and $x = 0$ (mV)	
$A(x,t)$	Amplitude of acoustic pulse a time t after emission and corresponding distance x from the source (mV)	
$G(x)$	Spreading loss a distance x from the acoustic source (dB/m)	
k	Wavenumber of acoustic wave (m^{-1})	
$A(x)$	Amplitude of acoustic pulse a distance x from the source (mV)	
Q	Quality factor (dimensionless)	
π	pi (dimensionless)	
E	Mean energy per cycle of oscillation (joules)	
ΔE	Energy lost per cycle (joules)	
v_p	Phase velocity (m/s)	
f	Frequency (Hz)	
$A(f)$	Amplitude spectra (dimensionless)	
R	Reflectivity of an impedance boundary (dimensionless)	
T	difference in two-way time between two sediment interfaces (ms)	
m	Gradient (V/Hz)	
X	difference in distance travel by two signals (m)	
Q_t	Quality factor of test medium (dimensionless)	
Q_r	Quality factor of reference medium (dimensionless)	
v_t	Phase velocity of test medium (m/s)	
v_r	Phase velocity of reference medium (m/s)	
f_j	Central frequency of jth passband (Hz)	
$A_a^j(f)$	Root-mean-square energy of jth passband of windowed attenuated signal (Joules)	
$A_r^j(f)$	Root-mean-square energy of jth passband of windowed reference signal (Joules)	
t_{ref}	Two-way time of reflectorsms (ms)	
ζ	Set of variable Q and t$_{ref}$ parameters (dimensionless)	

$S(\zeta)$	Difference function (dimensionless)
$F(t,\zeta)$	Theoretical value predicted for parameter set ζ and at time t (mV)
$M(t)$	Observed value at time t (mV)
T_r	Start of window of reference signal (ms)
T_a	Start of window of attenuated signal (ms)
$x(t)$	Received signal, as a function of time t (mV)
$\hat{x}(t)$	Quadrature of received signal as a function of time t (mV)
n	Integer, representing time instant (dimensionless)
$IF(n+\frac{1}{2})$	IF at time $t=(n+1/2)\tau_s$ (Hz)
$x(n)$	real signal at time $n\tau_s$ (mV)
$\hat{x}(n)$	quadrature of signal at time $n\tau_s$ (mV)
$dx(n)$	$x(n+1)-x(n)$ (mV)
$d\hat{x}(n)$	$\hat{x}(n+1)-\hat{x}(n)$ (mV)
$S(t,f)$	Coefficients of STFT at time t and frequency f (dimensionless)
$w(\tau-t)$	Windowing function (dimensionless)
$WVD(t,f)$	WVD coefficients at time t and frequency f (dimensionless)
$r(t,\tau)$	Correlation function
$K^q(n,m)$	q^{th} order PWVD kernal (dimensionless)
b_k, c_k	Coefficients of PWVD kernal (dimensionless)
$fshift$	Gradient of linear least-squares fit applied to IF data (Hz/ms)
k	Parameter which controls effect of sediment type on attenuation (dB/ms/Hz)

Greek letters

ω	Angular frequency of acoustic wave (rad/s)
τ_s	Sampling interval (ms)
α_n	Intrinsic attenuation coefficient (Nepers/m)
α_{dB}	Intrinsic attenuation coefficient (dB/m)
λ	Wavelength of acoustic wave (m)
τ	Relaxation time (s)
δ	Logarithmic decrement (dimensionless)
α_n^j	Attenuation of jth passband (Nepers/m)

$\phi(t)$ Phase of complex signal at time t (degrees)

τ_j Time shift of cross-correlation maximum of jth passband (ms)

ζ Set of variable Q and t_{ref} parameters (dimensionless)

$\sigma(t)$ Analytic signal as a function of time t (mV)

$\sigma(\tau)$ Analytic signal at lag τ (mV)

$\sigma_{ob}(t-\tau/2)$ Analytic observed signal at time t and tag $\tau/2$ (mV)

$\sigma_{ref}(t-\tau/2)$ Analytic reference signal at time t and tag $\tau/2$ (mV)

$\sigma(n+c_k m)$ Analytic signal at time $n\tau_s$ and lag $m\tau_s$ (mV)

1. Introduction.

The geotechnical and geoacoustic properties of marine sediments are of fundamental importance to a wide suite of marine fields. The properties which this report will focus on are compressional wave velocity and attenuation. These properties, if combined with additional physical information, *e.g.* porosity and density, can be used to estimate many additional physical and acoustic parameters, such as frame and bulk moduli. These estimations are primarily done using empirical equations or regressions (Richardson and Briggs 1993). Compressional wave velocity and attenuation also control the manner in which sound interacts with the seafloor, and hence are applicable to military sonar performance studies. They can be used to assess the stability of seafloor sediments (Sills, Wheller et al. 1991), which is important in predicting submarine landslides and locating sites for oil rigs. They can also be used to identify hydrocarbon reservoirs (Sheriff and Geldart 1995) and hence have commercial applications in the prospecting of energy resources.

A variety of techniques can be used to measure geoacoustic properties of marine sediments. Laboratory techniques involve the collection of sediment samples, through grab sampling or coring and subsequent analysis in the laboratory. This has several limitations. Firstly the relatively small sample volumes that are collected limit the analysis to high frequencies, typically over 100 kHz. Secondly the collection, transport and storage of the samples will disturb the sample in a manner which cannot be predicted. Hence even if *in situ* pressure of the sample is maintained during collection, transport and storage (Tuffin 2001) or such pressures and temperatures are simulated (McCann, Sothcott et al. 1998) the resulting measured geoacoustical properties cannot be directly related to the sediments *in situ*.

Alternatively geoacoustcal parameters can be estimated from *in situ* acoustic data. This possesses the advantage that any sediment disturbance is minimised. In addition the volume of sediment examined can be controlled and hence the acoustics of lower frequencies can be investigated. *In situ* acoustic data can be collected using two possible techniques.

- **Reflection techniques.**

Reflection techniques traditionally involve using an acoustic profiler located at the water surface to propagate an acoustic pulse into seabed sediments. The reflected waves are then detected by acoustic sensors situated near the water surface. Depending on the profiler employed the emitted signal can be monotone or broadband, and can impact the seabed at close to normal incidence, or a range of incidence angles. Frequencies used depend on the source but are typically below 15 kHz. The profilers and sensors are normally towed behind a surface vessel, thus allowing the profiling of a wide region of undisturbed seafloor sediment in a single survey. Resolutions

obtained depend on the profiler, e.g. the normal incidence chirp profiler can obtain *vertical* resolutions on the decimeter scale in the top c. 30 m of unconsolidated sediment and *horizontal* resolutions of approximately 1 - 2 m (Quinn 1997). Simultaneous acquisition from several parallel rows of streamers, *i.e.* long lines of acoustic sensors, enables the production of 3-D images of the sediment subsurface (Kearey and Brooks 1991). Reflection techniques can be applied to shallow/deep-water sediments.

- ### *In-situ* transmission techniques.

In situ transmission techniques involve the positioning of acoustic sources and receivers in marine sediments. A suite of devices allows the full range of sediment environments to be examined, from land/inter-tidal sediments to deep-water sediments. The acoustic signal transmitted from the source to the receivers is collected and analysed. Sediments under examination will experience some disturbance through the insertion of the acoustic devices. However if sufficiently large transmission paths are used, these disturbances should have negligible effect. Transmission techniques are essentially 1-D spot tests, with many such surveys required to achieve any form of "3-D" image.

Both monotone and broadband sources can be used, with frequencies generally limited to less than 50 kHz. Individual surveys typically using only a finite number of frequencies over a limited frequency range, which is primarily due to technological reasons.

The purpose of this report is to review and improve present techniques available for the estimation of compressional wave velocity and attenuation, or Q values, from broadband acoustic data.

Section 2 discusses the propagation of acoustic waves through marine sediments, as this must be fully understood in order to review and modify present techniques. Section 3 reviews techniques that have been used to estimate the compressional wave velocity and attenuation from broadband acoustic data. Section 4 examines the application of Instantaneous Frequency techniques to chirp reflection data, thus allowing the optimum estimation technique to be selected.

II. Acoustic wave propagation in marine sediments.

This section will summarise the general theories behind compressional wave velocity and attenuation of marine sediment.

Theories governing velocity

The velocity estimation techniques discussed here are based on relatively simple concepts. They assume that the distance x travelled by certain components of the received signal is known and focus on accurately estimating the time taken t to do so:

$$v = \frac{x}{t}.$$ (1)

If broadband signals are being examined the velocity obtained depends on which component of the signal is under investigation. The use of individual frequency components results in the estimation of phase velocities, while the examination of the whole signal results in a group velocity.

Velocity estimators based on equation 1 cannot be applied to reflection data, a result of the depth of sub-surface reflection horizons reflections being generally unknown. The use of spatially frequent coring may help to alleviate, but not solve, this problem.

In the case of *in situ* transmission data the distance travelled by the directly transmitted wave is accurately known and so these techniques can be used. One approach of estimating the arrival time is to detect the first arrival of the directly transmitted signal above a threshold level. Alternatively if the source pulse, or another reference pulse, is available, the received signal can be correlated with this. The time at which the correlated signal peaks represents the first arrival time.

Theories governing attenuation

For a real source wavelet propagating into an attenuating, or inelastic, medium the amplitude A of the wave a distance x from the source and time t after emission is:

$$A(x,t) = A_O G(x) e^{-\alpha_n x} e^{i(kx - \omega t)}$$ (2)

where A_o is the amplitude of the wave at $t = 0$ and $x = 0$, $G(x)$ represents geometric spreading, ω is the angular frequency of the wave, k the wavenumber and α_n the intrinsic attenuation coefficient in units of inverse length/m, or nepers/m. The spreading term is usually assumed to take the form of spherical spreading or cylindrical spreading, neither of which may be completely accurate. The intrinsic attenuation coefficient denotes the loss of power per unit distance and will be used extensively in the rest of this report. This includes the effects of scattering, absorption, and diffraction losses.

The intrinsic attenuation α_n of the medium, in Nepers/m, can be calculated (Johnstone and Toksoz 1981) from:

$$\alpha_n = \frac{1}{x_2 - x_1} \ln \left[\frac{A(x_1)}{A(x_2)} \cdot \frac{G(x_2)}{G(x_1)} \right].$$ (3)

where $A(x_1)$ and $A(x_2)$ are the amplitude of waves that have propagated through distances x_1 and x_2 repectivelly, with $x_1 < x_2$, and $G(x_1)$ and $G(x_2)$ account for geometric spreading effects at these distances. Alternatively the intrinsic attenuation coefficient can be measured in dB/m using equation 4, while equation 5 allows α_n to be converted to α_{dB} using a basic conversion constant.

$$\alpha_{dB} = \frac{1}{x_2 - x_1} 20 \log \left[\frac{A(x_1)}{A(x_2)} \cdot \frac{G(x_2)}{G(x_1)} \right].$$ (4)

$$\alpha_{dB} = 20 \log(e) = 8.686 \alpha_n.$$ (5)

The Quality factor, or Q value, is an additional measure of energy loss that has widespread use in both mechanics and acoustics. It represents the inverse fractional energy loss per cycle, *i.e.* is defined by $2\pi.E/\Delta E$, where E is the mean energy per cycle of oscillation and ΔE is the energy lost per cycle. In the case of acoustics this is equivalent to equation 6, where λ represents the wavelength:

$$Q = \frac{2\pi}{1 - e^{-2\alpha_n \lambda}}.$$ (6)

It is important to note that the intrinsic attenuation coefficient and the Q value are equally valid measures of attenuation and the actual parameter estimated from acoustic data depends on the analysis technique used. The majority of the techniques discussed in this report focus on the estimation of Q.

Relevant research

For saturated sediments the majority research implies that velocity is independent of frequency, over the range of kHz to MHz, (Hamilton 1972). However, this is contradicted by recent work which has observed a significant amount of velocity dispersion in seafloor sands from 50 Hz to 50 kHz (Stoll 2002).

Over the frequency range of kHz to MHz, the intrinsic attenuation in dB/m is found to have a frequency dependence that is approximately linear, (Figure 1), (Hamilton 1972; Hamilton 1979; Buckingham 2000). However, with the present data available one cannot statistically differentiate between this linear relationship and frequency dependences which possess slightly different exponents, *e.g.* between f^1 and $f^{1.12}$ for fine grained sediments (Bowles 1997). The implied linear relationship between intrinsic attenuation, in dB/m, and frequency confirms that the dominant attenuation mechanism in marine sediments is absorption, a consequence of the wavelengths over

the frequency range of a few Hz to several hundred kHz being much greater than the grain size, and hence negligible Rayleigh scattering occurring (Hamilton 1972). If Rayleigh scattering were a dominant attenuation mechanism α_{dB} would be related to the fourth power of frequency.
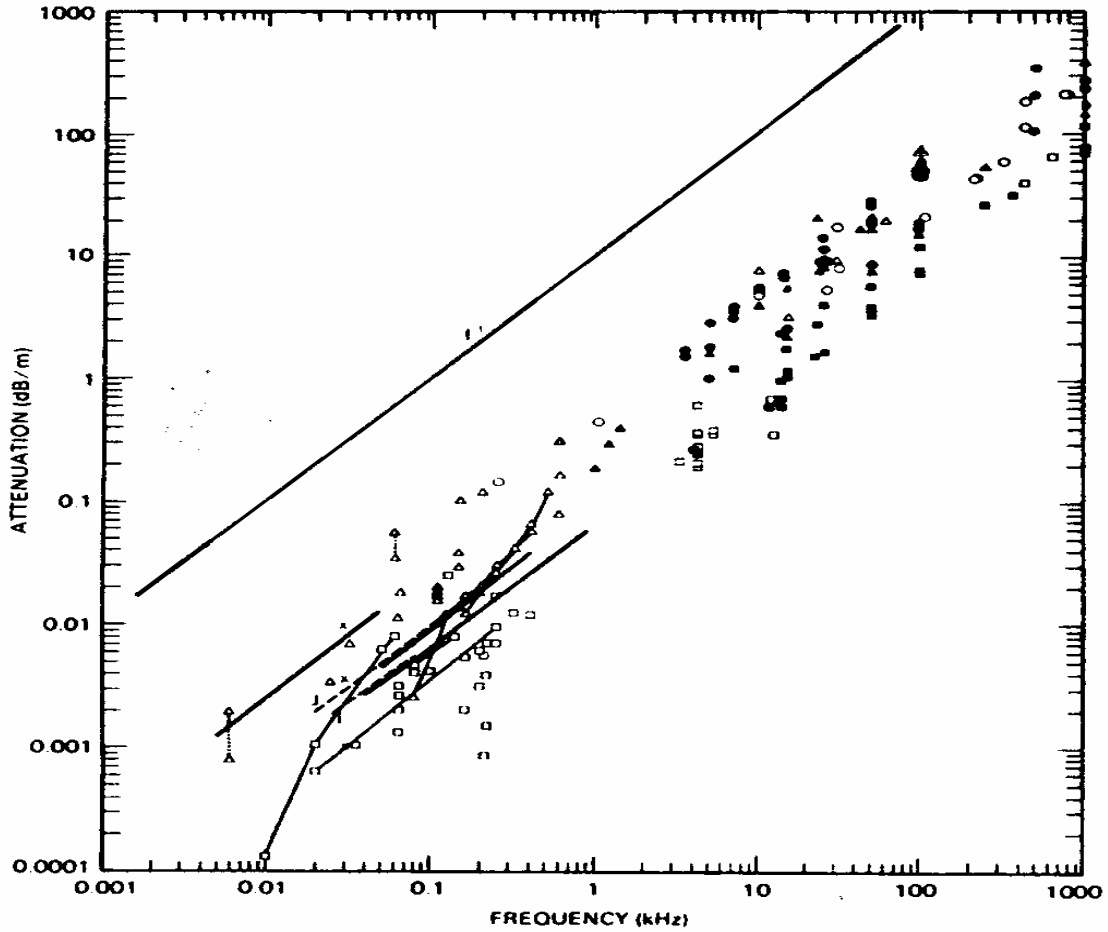
Figure 1: Attenuations of compressional waves in water saturated sediments and sedimentary strata: symbols denote measurements in different sediment types; shorter lines denotes fits applied to certain data sets and the longer line indicates a linear relationship. (From (Hamilton 1987)).

Though a Hookean, or elastic, model accurately accounts for the compressional and shear wave velocities of saturated sediments, it cannot account for the frequency dependence of the attenuation. This is because it neglects the relative motion of the pore water and mineral structure, which is a dominant attenuation mechanism. A viscoelastic model must be implemented if the attenuation is to be modeled accurately (Hamilton 1972). Most water saturated sediments qualify as media with "small damping" and so the exponential in equation 6 can be expanded as a series with only the first order term retained, (Hamilton 1972):

$$\frac{1}{Q} = \frac{\alpha_n v_p}{\pi f} = \frac{\delta}{\pi}. \tag{7}$$

15

where v_p is the phase velocity, f is the frequency and δ is the logarithmic decrement, an additional measure of attenuation. In the case of an attenuation which varies linearly with frequency Q will be independent of frequency.

For partially saturated, or gassy, sediments the above trends and models do not hold. The frequency dependence of compressional wave velocity and attenuation are much more complex, both of which depend on the resonant frequency of the gas bubbles present. A model of gassy sediments has been developed (Anderson and Hampton 1980; Anderson and Hampton 1980). Application of this to *in situ* gassy sediments resulted in the model allowing a broad classification of attenuation, with discrepancies between the modeled and measured attenuation explained by the omission of diffusivity effects and assumption of spherical bubbles in the model (Tuffin 2001).

One can see that in order to examine the full range of marine sediments an estimation technique used should be able to handle attenuations which vary both linearly and non-linearly with frequency.

III.   Present analysis techniques available for broadband data.

This section will review present published techniques that can be used to estimate the compressional wave velocity and attenuation from broadband acoustic data. Not all of the techniques present in literature will be thoroughly examined, with the following techniques being disregarded in favour of other more promising techniques.

- Rise time method: this technique is highly unstable in the presence of noise and requires essentially noise free data. Any form of field data does not fulfil this requirement (Jannsen, Voss et al. 1985; Tarif and Bourbie 1987);

- Inverse Q filtering: the primary aim of Inverse Q filtering is the removal of attenuation effects from seismic data sets. Examination of this method found that it is essentially that of wavelet modelling, whose primary aim is the estimation of velocity and attenuation, or Q value. Hence inverse Q filtering will be discarded in favour of more applicable wavelet modelling techniques.

- Spectrum modelling: this is a technique that is very similar to wavelet modelling, but does not convert the modelled attenuated spectrum into the time domain before comparison, *i.e.* it directly compares the spectra of the observed and modelled data. Though this has the advantage that the Inverse Fourier Transform is not required, it disregards half the information present in the seismic data. Spectrum modelling is a by-product of wavelet modelling. If these two methods produce consistent results it can be assumed that the amplitude spectrum contains sufficiently accurate phase information and all absorption information. As this may not be the case, this method is discarded in favour of wavelet modelling;

IIIa Spectral ratio methods.

This technique has been used for many years by seismologists to analyse reflection, *in situ* transmission and laboratory data. It can be applied to monotone pulses or pulses with a finite bandwidth. The basic theory involves calculating the log-spectral-ratio (LSR) of two signals, i.e. the ratio of the Fourier Amplitude spectra of the signals, and relating this to the different degree of attenuation experienced by each signal. However, slightly different approaches are assumed depending on the data being analysed.

- *Reflection data.*

Here the two signals being analysed will be the reflections from two different interfaces at two different depths. This is specifically discussed in Jannsen *et al.* (1985) and results in the following relationship between signals reflected from interfaces at depths x_1 and x_2:

$$\ln\left(\frac{A(f)_1}{A(f)_2}\right) = \ln\left|\frac{G(x_2)}{G(x_1)}\right| + \ln\left|\frac{R_2(1-R_1^2)}{R_1}\right| - 2\alpha_n(x_2 - x_1). \tag{7}$$

where $A(f)_1$ and $A(f)_2$ are the amplitude spectra of the wavelets reflected at depths x_1 and x_2 respectively, $G(x_1)$ and $G(x_2)$ are the corresponding geometric spreading coefficients, R_1 and R_2 are the corresponding reflection coefficients and α_n is the intrinsic attenuation coefficient of the intermediate layer, in nepers/m. Under the assumption that the geometric spreading and reflection coefficients are independent of frequency, and substituting for α_n from equation 6, this converts to:

$$\ln\left(\frac{A(f)_1}{A(f)_2}\right) = const + \frac{fT}{2}\ln\left(1 - \frac{2\pi}{Q}\right) \tag{8}$$

where T is the difference in the two-way travel times to each reflector. This allows the spectral ratio for discrete points in the spectrum to be plotted against f. For Q independent of frequency this plot is a straight line and the Q value can be calculated from the gradient m_1 through the equation:

$$Q = \frac{2\pi}{\left[1 - e^{(2m_1/T)}\right]}. \tag{9}$$
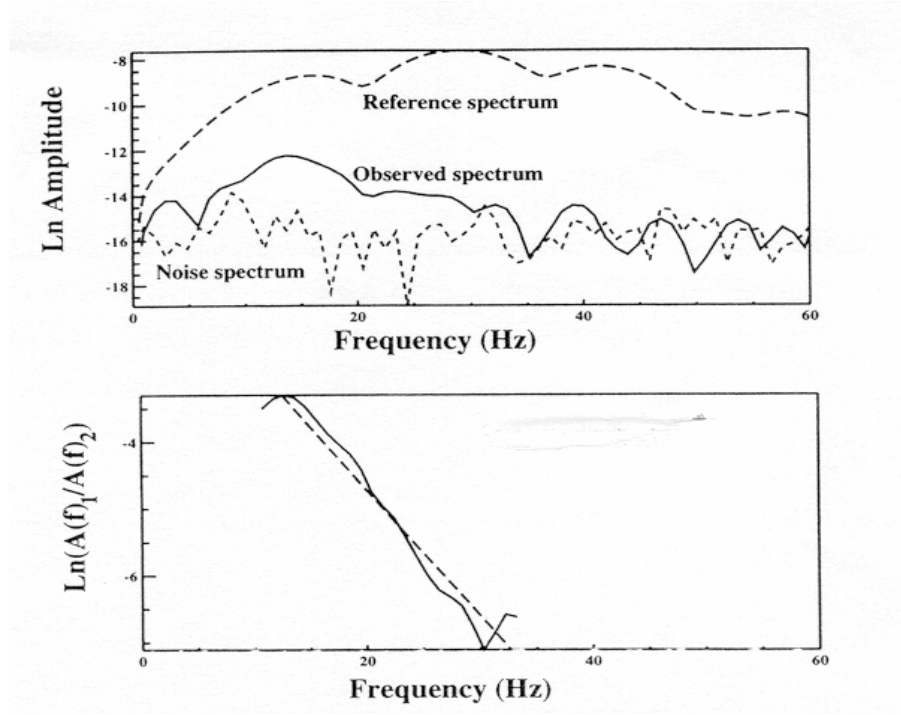
Figure 2: Application of spectral ratio method to reflection data:
Upper diagram displays spectra of reference pulse, i.e. that reflected at depth x_1, and the observed spectrum, i.e. that reflected at x_2.
Lower diagram displays spectral ratio and linear fit applied.
(From (Matheney and Nowack 1995)).

- *In situ Transmission data.*

In order to use the spectral ratio method on *in situ* transmission data, it is necessary to have data from two receivers at known distances x_1 and x_2 from the source. The LSR of these signals can be related to the Q value of the sediment using equation 9:

$$\ln(A(f)_1 \big/ A(f)_2) = const + \frac{X}{2v_p} f . \ln\left(1 - 2\pi \big/ Q\right). \tag{10}$$

where $X=x_2-x_1$ and $A(f)_1$ and $A(f)_2$ represent the amplitude spectra of signals received at distances x_1 and x_2 from the source. As before this allows the spectral ratio for discrete points in the spectrum to be plotted against f, which will form a straight line if both v_p and Q are independent of frequency. The Q value can be calculated from the gradient m_2 as described below:

$$Q = \frac{2\pi}{\left[1 - e^{\left(2v_p m_2 / \Delta x\right)}\right]}. \tag{11}$$

An inherent problem of any spectral ratio technique is the assumption that velocity is independent of frequency and attenuation varies linearly with frequency, i.e. the Q value is independent of frequency. This limits the validity of the technique to saturated sediments.

In addition the original spectral ratio method is not applicable to interfering signals. A modified version, which uses the Smoothed Pseudo Wigner Ville distribution and excludes the frequencies at which interfering signals overlap, has been developed (Maroni and Quinquis 1997). However this was only tested on synthetic data and concludes that though the new technique reduces the error when overlapping signals are present, it is not yet valid.

For noise free data collected in the laboratory, the best accuracy for the spectral ratio method is for intermediate Q values ($5<Q<50$). The method is less accurate for $Q<5$, which corresponds to highly attenuated signals, and highly inaccurate for $Q>50$, where the slope of the spectral ratio curve is nearly flat (Tarif and Bourbie 1987). As a comparison typical Q values of saturated sediments and sedimentary rocks range from $10 - 100$, while Q values of gassy sediments are typically less than 10.

Tests on synthetic data demonstrate that "the spectral ratio method is reliable in the presence of strong noise" (Tarif and Bourbie 1987), while Jannsen *et al.* (Jannsen, Voss et al. 1985) note that the lateral reflections and coupling problems "could well lead to erroneous measurements of Quality factors".

It may be possible to modify this technique to include Q values that vary slowly with frequency. This can be attempted by dividing the frequency axis into intervals of width Δf, assuming that Q is independent of frequency over Δf and imposing a linear fit to the data in each interval. The Q value of frequencies in this interval can be calculated from the gradient of the linear fit, as described previously. This is limited by the increment between recorded frequencies.

IIIb   Use of Instantaneous Frequency and spectral shift.

This method uses the preferential attenuation of high frequency components, and the subsequent shift in the central frequency of a broadband source, to estimate the attenuation (LeBlanc, Panda et al. 1992; Panda, LeBlanc et al. 1994). Though the following discussion applies the Instantaneous Frequency technique to chirp reflection data, the method can also be applied to *in situ* transmission data.

The *first stage* is to use a single relaxation time theory to model shifts in central frequency. The relaxation time of the media is the finite time necessary for a sudden change in pressure, such as a sound field, to translate into a density change. Different attenuation processes will exhibit different relaxation times. The single relaxation theory assumes that marine sediment is macroscopically homogeneous and its many different relaxation times can be represented by a mean relaxation time. In first order approximation this results in the frequency dependent intrinsic attenuation coefficient α_n, measured in nepers/metre :

$$\alpha_n = \frac{2\pi^2 f^2 \tau}{v_p}.$$ (12)

where v_p is the compressional wave phase velocity, f is the frequency and τ is the relaxation time.

LeBlanc *et al.* (1992) use equation 12 to convert measured attenuations from the literature into relaxation times (Figure 3). These attenuations were measured in a range of saturated sediment types and environments. Measurements at frequencies less than 50 kHz were made using *in situ* probes, while measurements at higher frequencies involved the laboratory analysis of sediment samples. LeBlanc *et al.* argue that the reduction in scatter resulting from plotting relaxation time, as opposed to attenuation, against mean grain diameter, justifies the application of a single-relaxation time model to marine sediments.

A trendline is then applied to figure 3, from which typical relaxation times for the six general sediment types are obtained (Table 1).
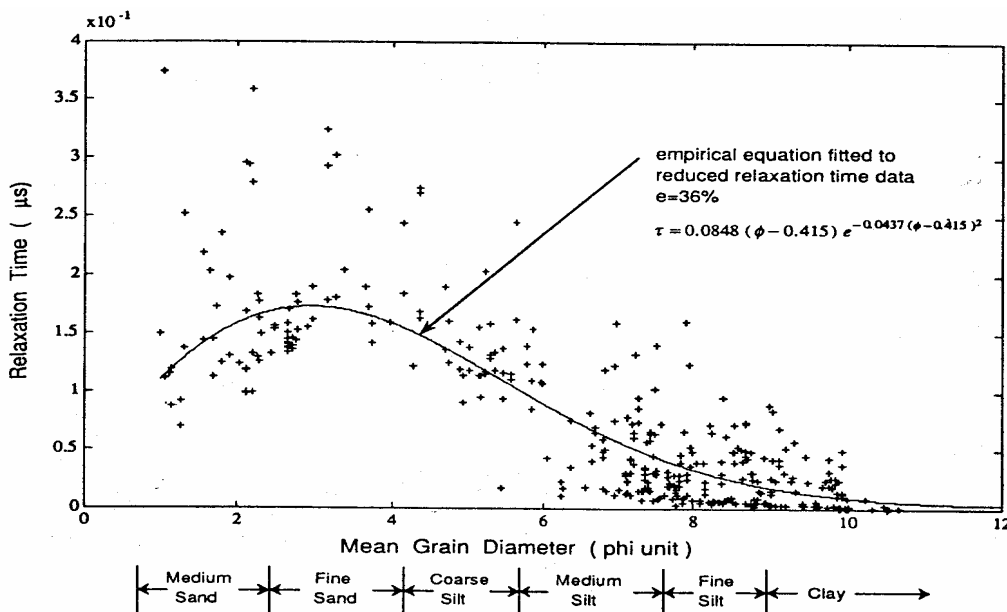
Figure 3: Attenuation measurements (from literature) converted into equivalent relaxation time and plotted as a function of mean grain size. (From LeBlanc *et al.*, 1991.)

Sediment type	Relaxation time(µs)
Medium Sand	0.15
Fine Sand	0.17
Coarse Silt	0.13
Medium Silt	0.06
Fine Silt	0.03
Clay	0.02

Table 1: Average relaxation times for different sediment types. (From Leblanc *et al.*,1991.)

The attenuation described in equation 12 is applied to a 2 - 10 kHz synthetic chirp pulse propagating through three of the sediment types listed in table 1, *i.e.* sand, silt and clay. A velocity of 1500 ms^{-1} is assumed. Analysis of the spectra allows the down-shift of the pulse's central frequency to be calculated (Figure 4). If a linear fit is assumed, a frequency shift per meter can be assigned to each sediment type. In order to obtain an empirical relationship between frequency shift per meter and relaxation time, this shift is plotted against the relaxation time (Figure 5). Note that the fit in Figure 5 is very poorly defined, as only three data points and the origin are used in its construction.
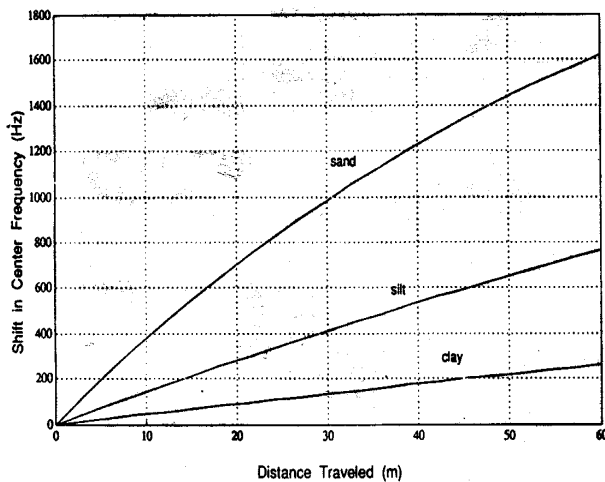
Figure 4: Relationship between shift in central frequency of pulse per metre and relaxation of sediment. (From LeBlanc *et al..*, 1991.)
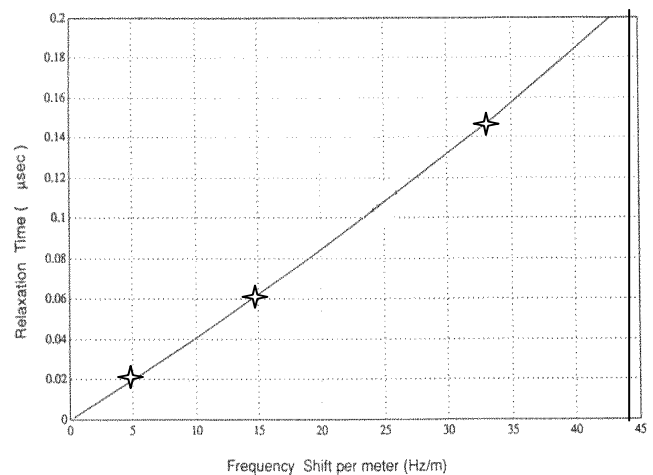
Figure 5: Modelled shift in 2-10 kHz chirp pulse for three general sediment types. (From LeBlanc *et al.,* 1991.)

The *second stage* calculates the frequency shift per meter observed from actual chirp reflection data. It uses the Instantaneous Frequency (IF) as an estimate of the central frequency of the received signal (Boashash 1992).

For a single trace this is calculated using the following method, the validity of which will be discussed in Section 4.b:

- Compression of the data, i.e. correlation of the received signal with the emitted chirp pulse, in order to improve resolution and SNR;
- Conversion of the compressed trace into a complex trace, using the Hilbert transform;
- Estimation of the IF from the phase of the complex signal $\phi(t)$ using equation 13, which is calculated numerically:

$$IF(t) = \frac{1}{2\pi} \frac{\partial \phi(t)}{\partial t}. \tag{13}$$

Estimations of IF can contain many anomalous points, a probable consequence of the unstable nature of IF. In the literature two approaches are used to remove such points. The first method involves calculating the IF for 20 adjacent traces individually and then stacking these IF series to form a composite IF which represents the section (LeBlanc, Panda et al. 1992). The second method selects only those points that possess a high SNR, i.e. points that correspond to the envelope peaks of reflections events with high SNR. For twenty adjacent traces, all such points above the 1st multiple are plotted against depth in sediment to obtain a composite IF (Panda, LeBlanc et al. 1994).

A best-fit line is then applied to the resulting IF plot, neglecting data in the vicinity of, and below, the first multiple. The gradient of this line is an estimate of the mean frequency shift per metre (see Figure 6). This is related to a relaxation time using the empirical relationship derived from Figure 5 and allows a sediment type to be assigned. Attenuation can then be calculated using equation 12.
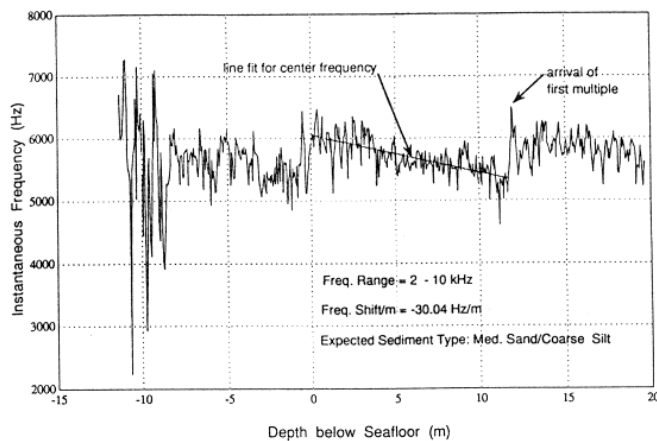
Figure 6: Estimation of frequency shift per meter and assignment of sediment type. (From LeBlanc *et al.*, 1992).

The IF spectral shift technique possesses an inherent problem. It assumes that all attenuation mechanisms present in marine sediment can be classified by a single relaxation time. This assumption is used in the estimation of relaxation time from seismic data and, if not applicable to the sediment under examination, will result in incorrect assignments of relaxation time. Hence the estimation of attenuation will also be incorrect. In addition the attenuation is assumed to increase with the square of frequency, with the justification of this assumption being unconvincing. This contradicts previous research into compressional wave attenuation, which implies a linear relationship (Section 2).

The assignment of sediment type by this method is also ambiguous. This is due to the non-monotonic nature of the trendline in Figure 3, which relates relaxation time to mean grain size, *e.g.* a relaxation time of 0.15 μs may correspond to coarse silt or medium sand. Even if this is only used to classify silts and clays the wide scatter from the trendline makes such classifications unreliable.

LeBlanc *et al.* (1992) compares the sediment type predicted using the IF technique to core samples for seven sites in Narragansett Bay, Rhodes Island. Predictions of sediment type are generally within 1 sediment group of that observed in the core sample, *e.g.* IF predicts a fine sand while the core sample displays a coarse silt. Panda *et al.* (1994) use synthetic data, and so offer no evidence that the techniques work well with real data. However, both papers provide no quantitative assessment of the IF techniques used.

A comparison of spectral ratio and IF techniques, using IF values at envelope peaks only, on 5 - 30 kHz *in situ* data concludes that the IF method applied by Dasios *et al.* " is more robust and suitable to the application of sonic waveform data" (Dasios, Astin et al. 2001). It is noted that this is possible because IF measurements are based on one stable point only, and so are less affected by secondary arrivals. Spectral ratio techniques are based on the whole spectrum and will be affected by secondary arrivals.

Finally, both methods of removing the scatter in IF involve an effective stacking of twenty adjacent traces. Assuming a survey speed of 4 knots (2 m/s), and using a typical pulse rate of 4 per second, this corresponds to approximately 10 m. This will limit the effective horizontal resolution of this technique.

IIIc Filter correlation techniques.

The filter correlation technique involves two stages. First the received signal is bandpass filtered and then it is correlated with the source wavelet. If the source to receiver separation is known this allows the simultaneous estimation of a frequency dependent attenuation and velocity.

The method discussed below is an adaptation of the filter correlation method developed by Courtney and Mayer (Courtney and Mayer 1993), which was used by Best *et al.* (2001).

The filter correlation method requires a reference signal and an attenuated signal. Typical reference signals include the signal emitted by a repeatable source and, for *in situ* transmission, the signal received at the smallest source to receiver separation. Both the reference and attenuated signal are over-sampled in time, with respect to the Nyquist frequency, in order to allow accurate temporal resolution in the correlation step. In addition both signals are windowed in time. This helps to remove noise and unwanted reflections. The symbols *Tr* and *Ta* denote the start times of the reference and attenuated windows, relative to the time instant at which the source signal was

emitted. These are calculated using simple threshold conditions. A final pre-processing stage used by Best *et al.* [2001] is to compensate for cylindrical spreading losses.

The first processing step involves filtering both the reference and attenuated signal in the frequency domain. This separates the data into *n* bands, with the central frequency of the *j*[th] passband denoted by f_j (e.g. Best *et al.* (2001) use 14 passbands). This is implemented using a causal filter (*e.g.* Butterworth filter) to prevent the energy of secondary arrivals migrating back in time.

The second step entails a cross-correlation between the reference and attenuated waveform in each passband. The velocity is estimated using a time shift τ_j, corresponding to the cross-correlation maximum of the *j*[th] band, equation 14, (with one half period of zero time shift to avoid phase wrapping, where the period is $1/f_j$).

$$v^j = \frac{\delta x}{T_a - T_r + \tau_j} \tag{14}$$

The attenuation coefficient α_n^j for the *j*[th] passband can be calculated using:

$$\alpha_n^j = \frac{1}{X} \ln\left(\frac{A_a^j(f)}{A_r^j(f)} \right). \tag{15}$$

where X is the difference in the distance traveled between the reference and attenuated waveform, and $A_a^j(f)$ and $A_r^j(f)$ are the root-mean-square energy of the windowed attenuated and reference signals in passband j.

As this technique allows the frequency dependence of velocity and attenuation to be estimated without presuming any geoacoustic models, it can be applied to both saturated and gassy sediments. However the distance traveled by the attenuated signal needs to be known. Hence filter correlation can be readily applied to transmission surveys. In order to apply filter correlation to reflection surveys the compressional wave velocity profile must first be obtained from independent sources.

Both techniques were tested on synthetic noise free data, which was generated with a specific attenuation. These tests display how filter correlation techniques can accurately estimate attenuation for much smaller windows (i.e. those greater than 15 µs) than Fourier techniques can (i.e. those greater than 25 µs) (Courtney and Mayer 1993). In the case of synthetic data they "confirm the stability and accuracy of filter correlation method … in the presence of 2nd multiples" (Courtney and Mayer 1993).

One point of concern is the manner in which Courtney and Mayer (1993) calculate the central frequency of each band. This is estimated using the mean zero-crossing interval. It is noted

that this produces a very rough estimate of the mean frequency. Better estimates may be obtained by using the mean frequency of each band (Best, Higgett et al. 2001).

IIId Wavelet modeling.

In wavelet modeling, synthetic seismograms are calculated for a range of varying parameters and a best fit is found with observed seismic data. The simple application to a single arrival on a seismogram is described in Jannsen *et al.* (1985). The wave incident on the water-sediment interface, which is denoted by $x = 0$, is used as a reference wave. This automatically removes any errors that may be introduced through either the transmission of the signal from the profiler or the transmission of the signal through the water column and overlying sediment layers.

The spectrum of the reference wave can be used to produce synthetic seismograms for reflectors located at a range of two-way times t_{ref} and frequency dependent Quality factors Q. These frequency dependent Quality factors will be the result of an assumed attenuation model. Wavelet modeling then back-transforms the spectral information into the time domain, typically using an Inverse Fourier Transform. The synthetic seismograms are compared to the observed data, with the best fit values of Q and t_{ref} resulting in the minimum of the function $S(\zeta)$:

$$S(\zeta) = \sum_k \left| F(t,\zeta) - M(t) \right|.$$

(16)

where $F(k,\zeta)$ is the theoretical value at time t and parameter set $\zeta=(Q,T)$ and $M(t)$ is the observed value at time t.

The calculation of the cross correlation of the modeled and observed signals may provide an alternative manner of estimating the best fit parameters, i.e. the best fit parameters correspond to the maximum cross correlation. In order to conserve computational time it is necessary to limit the variation of t_{ref} to a "reasonable time-interval." Hence a rough estimate of t_{ref} should be known. This is calculated from the covariance of seismograms (calculated for Q values chosen roughly equidistant on a logarithmic scale) and the reference signal, with a relative minimum indicating a relatively good temporal fit between the major reflections (Jannsen, Voss et al. 1985). However it may be possible to estimate t_{ref} using IF events, which supplies an unambiguous and robust manner of identifying the first arrival from a reflection (Taner, Koehler et al. 1979).

The above method assumes that the velocity is known. However it could easily be modified to allow velocity and Q value to become the two unknown variables, by simply calculating t_{ref} using the IF events and assuming this to be a constant in the attenuation models used.

A comparison of four techniques by Jannsen et al (1985) (rise time, spectral ratio, wavelet and spectrum modeling) concludes that for real data the modeling techniques result in significantly

less scatter than other methods. However care must be taken during the application of the initial constraints on t_{ref} as these will affect results dramatically.

IIIe Conclusions.

The desirable features of a technique that can be used to estimate the attenuation and velocity of seafloor sediments from acoustic data are:

- It is robust in the presence of noise and overlapping reflections;

- It is able to incorporate frequency dependent velocities and Q values;

- It is independent of any *specific* geoacoustic models or theories, the use of which will limit the range of sediment types the technique is valid for;

Table 2 summarizes these properties for each of the techniques discussed in section 3.

Technique	Geoacoustic Properties assessed	Robust in presence of noise/overlapping reflections/	geoacoustic model assumed?	incorporates non-linear frequency dependence
Spectral ratio	Q	Possibly / No	Q independent of frequency	No
IF	α	Yes / Unsure	single relaxation-time theory	Possibly
filter correlation	Q, v	Yes / Yes	None	Yes
Wavelet modelling	Q, v	Yes / Yes	general attenuation	Yes

Table 2: Summary of techniques discussed in section 3.

In the case of reflection data the filter correlation method is not applicable, as the distances travelled by received pulses are unknown and can only be estimated through the use of modelling or ground-truthing cores. Spectral ratio posses the disadvantage that only media with frequency independent Q values can be examined. Both wavelet modelling and IF techniques appear more promising. However, it is possible that wavelet modelling may produce a variety of ambiguous results, all of which fit the data under examination. The use of Instantaneous Frequency requires some modifications, including:

- The use of a technique that accurately estimates the Instantaneous Frequency of reflection data;

- The use of attenuation equations, in the modelling stage and in the final calculation of attenuation, which are applicable to the sediments under examination;

For *in situ* transmission data the most promising technique appears to be filter correlation. This technique is permitted due to accurate knowledge of the distance through which the directly transmitted wave has propagated. Wavelet modelling and IF techniques also appear promising for *in situ* transmission data, with the concerns/modifications mentioned above.

IV   Application of selected techniques to reflection data.

It was decided to examine the application of the IF to reflection data collected from a chirp profiler, with efforts focusing on deducing the IF estimation technique which is most applicable to such data. Section 4.i. will discuss the main features of the chirp sub-bottom profiler and the specific datasets examined. Section 4.ii. investigates the fundamentals of IF and Group Delay estimates while section 4.iii. examines a variety of IF estimation techniques. The details of the application of the techniques are discussed in section 4.vi. and conclusions are presented in section 4.v.

IVa The chirp sub-bottom profiler.

The chirp sub-bottom profiler is a high-resolution, frequency-modulated, normal-incidence acoustic profiler. It emits a swept frequency pulse, which can incorporate a variety of FM laws (e.g. linear, quadratic and logarithmic) and span a frequency range of 1.5 – 15 kHz. An example of a 32 ms, linearly swept 2-8 kHz pulse is displayed in Figure 7. The chirp pulse permits better penetration than monotone surveying systems, without a significant reduction in resolution. The vertical resolution is "of the decimetre scale in the top c. 30m of unconsolidated sediments" (Quinn, Bull et al. 1998), and is dependent on the bandwidth of the source. The horizontal resolution depends on source characteristics (beam angle and dominant frequency), the compressional wave velocity of the sediments, the towfish altitude and the pulse rate of the system. Characteristic horizontal resolutions of 1 - 2m are obtained (Quinn 1997)

In order to achieve these resolutions the chirp pulse is compressed using a matched signal that correlates the chirp return signal with a replica of the "outgoing pulse" (LeBlanc, Mayer et al. 1992). The "outgoing pulse" used is the electronic pulse sent to the emitting transducers. This correlation produces a new effective wavelet, which is the auto-correlation of the outgoing pulse. The auto-correlation of the 32 ms, linearly swept 2 - 7 kHz pulse is displayed in Figure 8. As the correlation process squares the spectral amplitudes, the auto-correlated pulse possesses a sharper spectrum than the "outgoing pulse", An additional advantage of this correlation is that it achieves a signal processing gain over the background noise. Research by LeBlanc *et al* (1992) found that, in order to equal the performance of chirp sonar pulses, conventional pulse sonar would have to use a pulse with a peak power 100 times larger.

The chirp system is highly adaptable. It can be towed using a towfish or catamaran or deployed in an AUV. The reflected pulse is detected by hydrophone arrays, which have a frequency range of 0.5 - 15 kHz and contain piezoelectric receiving elements (Figure 9).
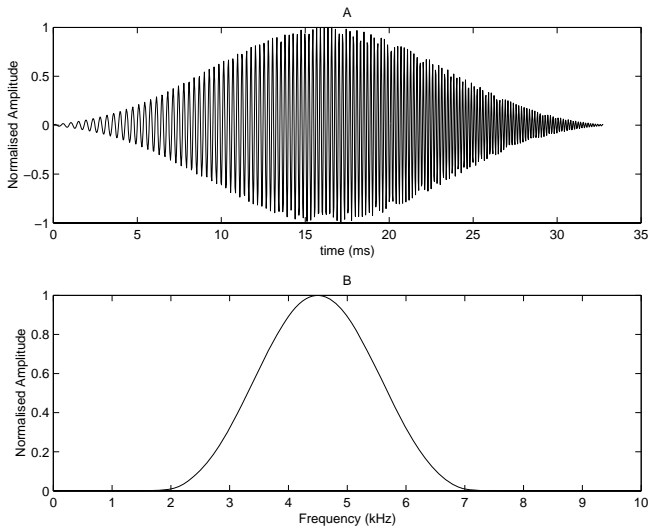

Figure 7: Properties of 32 ms, 2 – 7 kHz linearly swept "outgoing" chirp pulse: (A) time plot; (B) frequency spectrum.
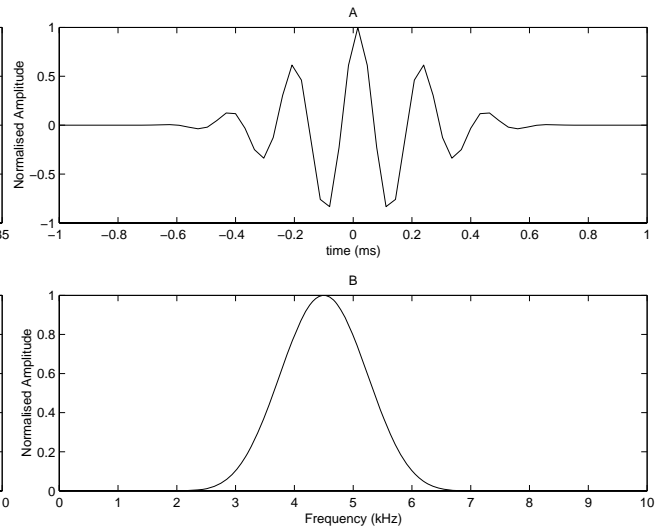
Figure 8: Properties of the autocorrelation of the 32 ms, 2 – 7 kHz linearly swept "outgoing" chirp pulse: (A) time plot; (B) frequency spectrum.
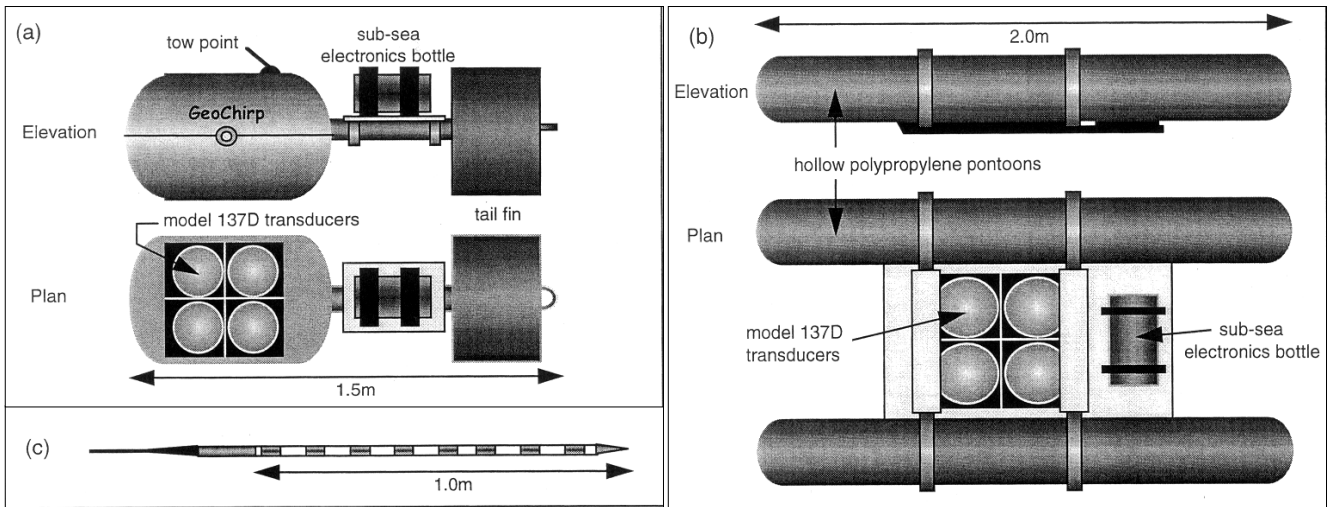
Figure 9: The main components of the Geaoacoustics GeoChirp acquisition system: (a) model 136A towfish; (b) catamaran deployment; (c) 8-section neutrally buoyant mini-streamer.
(From Quinn et al., 1998.)

Figure 10 shows a typical example of the data that is to be analysed. Each vertical line represents the received signal for a single emitted pulse after correlation with the chirp pulse. Dark shades represents sections of the trace that are greater than zero. The horizontal axis represents the trace number which can be related to a position using navigational data. This section displays several strong reflections that occur when the emitted chirp pulse encounters a boundary between

two media of different acoustic impedances. Both the seafloor reflection and additional subsurface reflections, occurring at the boundaries between sediment layers, are apparent. The first multiple reflection from the seabed is also marked.

Though chirp profiles can clearly identify geological interfaces, the estimation of the velocity and attenuation of sediment layers has proven more difficult. This is the aim of present research.
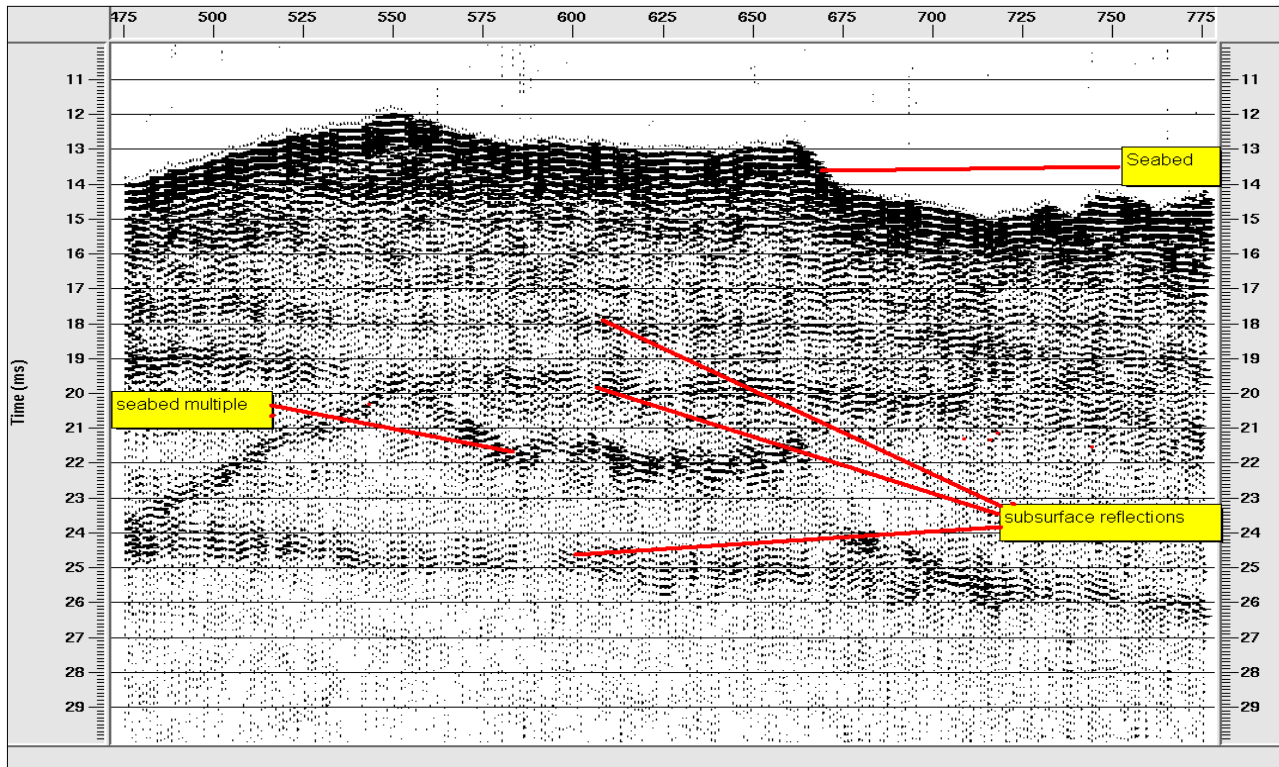
Figure 10: Typical chirp section (CDPs 475-775 of dataset collected from Bouldnor Cliff, Isle of Wight). Seabed, additional sub-surface layers and first multiple of seabed are marked.

Two chirp datasets from the South coast of England will be used in the following investigation. The first dataset was collected from Bouldnor Cliff, which lies on the NW coast of the Isle of Wight. The sediments in this area consist of Late Eocene material, e.g. marls and clays, underlain by Bembridge limestone at a depth of c. 22m (Dix, Jarvis et al. 2000). The second dataset was collected from Dibden Bay, Southampton Water. The sediment in this region consists of Holocene clays/silty clays, Pleistocene sands and gravels and Eocene bedrock (Robb 2000). Both physical and acoustic evidence of a widespread blanket of shallow gas has been observed (Tuffin 1997; Robb 2000)

Both datasets were collected using a 2-8 kHz linear chirp pulse, with duration of 32 ms and a pulse rate of 4/s.

IVb   Fundamentals of IF and group delay estimates.

The calculation of IF requires that the real seismic trace is first transformed into a complex trace. The complex trace used is the analytical signal $\sigma(t)$, which is constructed by treating the seismic trace $x(t)$ as the real part and its quadrature $\hat{x}(t)$ as the imaginary part. The quadrature is estimated using the Hilbert Transform (Boashash 1992):

$$\sigma(t) = x(t) + j\,\hat{x}(t) = A(t)e^{j\phi(t)}$$

(17)

The equation above displays how, at any time within the signal, it can be uniquely defined by a single amplitude A and phase ϕ, i.e. the instantaneous envelope and instantaneous phase.

The estimation of the complex signal obtained using the Hilbert transform will be sufficiently accurate if the spectra of the envelope function and phase of a signal do not overlap (Boashash 1992). If these spectra overlap the Hilbert transform will be the result of overlapping, phase distorted functions and will not correspond to the signal plus its quadrature component. The phase and envelope functions of the traces under examination are difficult to obtain and have little practical meaning. Hence we will consider these traces to be the convolution of the autocorrelation of the emitted pulse (Figure 8), with a simple reflectivity series, with additional noise components present. Hence if the spectrum of the envelope and phase of the autocorrelation do not overlap in frequency the Hilbert transform can be used to accurately construct the analytic signal. This condition is satisfied, with a phase spectrum containing frequencies from 2-7 kHz (Figure 8), and the envelope spectrum containing frequencies less 2 kHz. Hence the Hilbert transform is used to calculate the analytic signal. This is implemented discretely, as outlined in (Marple 1999), in order to correctly scale the DC and Nyquist Frequency terms.

As mentioned earlier the IF is simply the differential of the phase with respect to time (equation 14). For discrete data this differentiation can be calculated directly, using the convolution of the phase and the impulse function of a finite impulse response differentiating filter. However this results in the amplification of high frequency noise. Hence a variety of estimation techniques, each of which have different properties and subsequently result in slightly different estimation of IF have been developed (Boashash 1992). LeBlanc *et al.* (1992) and Panda *et al.* (1994) simply state that the IF was calculated numerically, which omits the critical matter of which technique was used. The optimum technique to use for chirp reflection data is examined in section 4.c.

In addition the Bandwidth-Duration product, or BT product, of a signal will affect our concept of IF. An alternative manner to estimate the frequency present in a signal is to use the Group Delay, *i.e.* find the time at which frequency f makes its maximum contribution to the signal. If the BT product is high, *i.e.* >10 (Boashash 1992), and the signal is monocomponent the

frequency estimate produced by IF and group delay methods will converge. If not, these two methods will produce different frequency estimates and raise the issue of which estimate is more realistic. As the correlated traces under examination are multicomponent and the BT product of the autocorrelation of the emitted wave, calculated using standard definations for B and T (Cohen 1995), is approximately 0.5, IF and group delay will produce different frequency estimates. This inconsistancy will simply be noted and the rest of the report will focus on the best manner of estimating the IF.

IVc Theory behind selected techniques.

Based on comprehensive research into IF (Boashash 1992; Boashash 1992; Boashash and O'Shea 1993; Boashash and O'Shea 1994; Ristic and Boashash 1996; Barkat and Boashash 1999) five basic estimation techniques were selected. Boashash states that, for linear chirps, techniques that use the moments of time frequency distributions are "computationally demanding … and not generally statistically optimal" (Boashash 1992). However the following work will examine both uncorrelated and correlated data and, as the correlation of the data reduces the linear chirp to a broadband signal, both peak and moment estimations of IF will be tested.

As the selected techniques include the use of both linear and quadratic time-frequency distributions (TFDs) it is necessary to examine the square of the TFD coefficients. This allows resulting IF estimates to be directly compared. The IF at a time t is calculated by analyzing the coefficients at that time, *i.e.* taking a time-slice through the distribution. The IF can be considered to be either the frequency at which the coefficients peak or the mean frequency (first moment) of the time slice. Both of these adaptations were tested for techniques that incorporate a TFDs.

The use of an alternative TFD, the Cross Polynomial Wigner-Ville Distribution, has been omitted owing to its highly intensive computational demands, *i.e.* it involves resampling to 10^5 times the original sampling rate (Ristic and Boashash 1996).

The following basic techniques were selected for testing.

- *The discrete classical time formula (DCTF)*. The DCTF estimates IF using the discrete differentiation of arctangent form of the phase, equation 18. It is extremely efficient to implement.

$$IF(n+1/2) = \left(\frac{1}{2\pi}\right) \frac{x(n).d\hat{x}(n) - \hat{x}(n).dx(n)}{x^2(n) + \hat{x}^2(n)}. \tag{18}$$

where *IF(n+1/2)* is the IF at the time instant $t_n=(n+1/2)\tau s$, with τs as the sampling interval and n an integer, *x(n)* and $\hat{x}(n)$ are the values of the real and imaginary parts of the analytic signal at t_n and *dx(n)* and *d$\hat{x}$(n)* are the differences between the *(n+1)*[th] and *n*[th] values of the real and

imaginary components of the analytical signal, i.e. *dx(n)=x(n+1)-x(n)* and $d\hat{x}(n) = \hat{x}(n+1) - \hat{x}(n)$

- *The peak and first moment of the short time Fourier transform (STFT).* The STFT is a linear TFD and is defined as the Fourier transform of windowed sections of a signal:

$$S(t,f) = \int_{\tau=-\infty}^{\infty} \sigma(\tau) w(\tau - t) e^{-2\pi 1 f\tau} d\tau. \qquad (19)$$

where *S(t,f)* are the STFT coefficients at time *t* and frequency *f*, *w(τ-t)* is the windowing function and *σ(τ)* is analytical signal at time lag *τ*. Both peak and first moment estimations of IF were investigated.

STFT estimations should perform well if the signal is quasi-stationary. However resolution limitations, which arise from the uncertainty principle, will produce poor results for rapidly varying signals (Boashash 1992).

- *The peak and first moment of the Wigner-Ville Distribution (WVD).* The WVD is the Fourier Transform of the instantaneous correlation function $r(t,\tau)$:

$$WVD(t, f) = \int r(t,\tau) e^{-2\pi i f\tau} d\tau . \qquad (20a)$$

$$r(t,\tau) = \sigma\left(t - \frac{\tau}{2}\right)^{*} \sigma\left(t + \frac{\tau}{2}\right). \qquad (20b)$$

where *WVD(t,f)* are the WVD coefficients at time *t* and frequency *f* and *σ(t)* is the analytic signal. This is implemented discretely by replacing *t* by $n\tau_s$, *τ* by $m\tau_s$ and the integral over *τ* to a sum over *m*, where *n* and *m* are integers and τ_s is the sampling interval.

The correlation function, which represents the kernel of this TFD, simply weights all lags equally. The WVD allows good localisation of energy and satisfies theoretical conditions. However it can be negative at some points, denoting a negative energy, and, owing to its quadratic nature, possess cross-terms. Hence it is of critical importance that the analytical signal is used, as this will reduce needless cross terms (Boashash 1988). IF is estimated using both peak and first moment methods, as described previously.

Using the peaks of the WVD is noted to be the optimum method for "high to moderate SNR signals which can be approximated well (at least locally) to linear FM signals" (Boashash 1992).

- *The peak and moment of the cross Wigner-Ville Distribution (XWVD).* The XWVD is formed in similar manner to the WVD, expect that the kernel used is the correlation function of the analytic observed signal σ_{ob} and an analytic reference signal σ_{ref}, i.e. equation 20b is replaced by:

$$r(t,\tau) = \sigma_{ob}\left(t - \frac{\tau}{2}\right)^* \sigma_{ref}\left(t + \frac{\tau}{2}\right). \tag{21}$$

An iterative approach is suggested (Boashash 1992), in which it is assumed that the reference signal is unknown and is calculated from the estimated IF of the observed signal. This is used to generate the XWVD and a new IF calculated from the peaks. A new reference signal is created and this process repeated until the difference in IF estimates from successive iterations is less than a specified amount. As the reference signal for a chirp profiler is both repeatable and accurately known this iterative procedure was omitted and the emitted pulse used as the reference signal. IF is estimated using both peak and first moment techniques.

"For low SNR non-stationary signals, which are comparatively long," the peaks of the iterative XWVD, generated using a sliding window, may supply a reliable estimate of the IF (Boashash 1992; Boashash and O'Shea 1993). However, the performance of the non-iterative approach used in this report is unknown.

- *The peak and first moment of the Polynomial Wigner-Ville Distribution (PWVD).* The WVD is similar to a central finite difference estimator and hence yields good energy concentration for noise-free linear FM signals. The PWVD incorporates a kernel that includes non-linear terms, with the general equation for a qth order PWVD kernel displayed below:

$$K^q(n,m) = \prod_{k=0}^{q/2} \{\sigma(n + c_k m)\}^{b_k} \{\sigma^*(n - c_{-k}m)\}^{-b_{-k}}. \tag{22}$$

where σ represents the analytic signal, b_k controls the weighting of different phase values, c_k controls the separation of different phase values used and n and m are the discrete versions of t and τ used earlier. The PWVD is simply the Fourier Transform of the above kernel.

The optimum settings for these constants have been deduced in (Boashash and O'Shea 1994) for a 4th order PWVD, i.e. one that can examine linear, quadratic, cubic and quadratic FM laws. These are listed below, along with the resulting kernel and are used in the subsequent analysis:

$$b_0 = 0; b_1 = -b_{-1} = 2; b_2 = -b_{-2} = 1$$

$$c_1 = -c_{-1} = 0.675; c_2 = -c_{-2} = 0.85$$

$$K^4(n,m) = \{\sigma(n + 0.675m).\sigma^*(n - 0.675m)\}^2.\sigma^*(n + 0.85m).\sigma(n - 0.85m). \tag{23}$$

Note that in order to form a discrete kernel the data must be resampled, to forty times its original rate. A frequency-scaled version of the kernel (Boashash and O'Shea 1994), which can be used to reduce errors that may arise during resampling has not been used due to its large computational demand, *i.e.* it would involve resampling to 1000 times the original rate. Again both peak and first moment estimates of IF are tested.

The PWVD peak based IF estimation performs well for polynomial phase laws, (Boashash and O'Shea 1994), with the IF estimation from the peaks of the PWVD out-performing other estimation techniques for signals with a SNR larger than 3 dB (Barkat and Boashash 1999).

IVd Data used and details of implementation.

The above techniques were applied to the two chirp datasets discussed in section 4.i. It is usual to compress the chirp pulse by correlating the signal received by the chirp profiler with the emitted pulse. However, as the performance of TFDs which incorporate correlations is not fully understood for reflection data, techniques were applied to both correlated and uncorrelated data. Note the XWVD techniques were not applied to correlated data, as these techniques inherently involve a correlation process. No geometric spreading corrections were applied to the traces, as application of such corrections usually assume basic spreading laws, which may not be completely accurate.

For each dataset 4 sections, of 9 traces each, were selected from both the correlated and uncorrelated data. The choice of 9 traces per section is an attempt to halve the section size used in previous IF research, while retaining a unique central trace to which composite results for the section can be compared. As the order in which the information from these traces is combined to produce a composite IF for the section is important, a variety of approaches were tested. These included the use of:

- The central trace, *i.e.* estimate the IF of the central trace of the section;
- Stacked traces, *i.e.* stack the traces to obtain a composite trace, from which IF is estimated;
- Stacked IFs, *i.e.* calculate the IF for each trace in the section individually, stack the IFs and normalize over the number of traces in the section. This is essentially the technique used by (LeBlanc, Panda et al. 1992), except a section of 9, rather than 20, traces is used;
- Stacked distributions, *i.e.* generate the relevant TFD for each trace in the section, square the coefficients and stack the resulting distributions. The IF is then calculated from the composite distribution;

Note that the absence of a TFD in the case of the DCTF prevents the use of the final approach for this technique.

As the manner in which the techniques were implemented is of paramount importance, particularly for those techniques based on the peaks of TFDs, such details will now be discussed.

Care was taken to ensure that almost all techniques produced IF profiles with the same theoretical frequency and temporal resolutions. These were set at 12.2 Hz and 0.04 ms, which were the most convenient values for the sampling frequency of the received data (25 kHz) and the

data length examined (2048 points). An exception is the DCTF, which theoretically has an infitesimally small frequency resolution. Note that this does not translate into an infinitely accurate value of IF, as the techniques which we are examine estimate IF.

In order to obtain these resolutions the following parameters were used:

- The number of frequency bins in each TFD was set to the number of data points under analysis.
- The TFDs used windows with maximum overlap.

In addition the STFT window size was set to 2.56 ms, to optimize it performance, and digital version of the 32 ms,

2-8 kHz linear chirp pulse used to collect both datasets, which was supplied by Geo-acoustics Ltd., was used as the reference pulse in the formation of the XWVD. Note that the only difference between the techniques is the degree of smoothing each one incorporates, with the XWVD, PWVD and WVD using maximum smoothing, the STFT using intermediate smoothing and the DCTF using no smoothing.

A final point is that the acquisition of data by the chirp system introduces a delay of approximately 3.5 ms. This has not been removed as the absolute depth of reflectors below the sea surface bears no relationship on the relaxation times and attenuations which will be estimated. If geometric spreading losses had been corrected for, or we wished to accurately locate the depth of the seabed or other sub-surface reflectors, it would be necessary to account for this time delay.

IVe Results and discussion.

The IF estimations obtained from the techniques and stacking methods discussed in section 4.iv. were examined. This was done with the aim of identifying the method which produces IF estimates that are most effective in the calculation of relaxation time, grain size and attenuation. Such a technique will ideally result in:

- An IF which varies smoothly with two-way time and clearly displays regions over which IF decreases linearly with two-way time;
- The two-way times at which these regions start and end corresponding to observed reflection events and hence to individual sediment layers;
- Relaxation times that are less than 0.2 μs. This value was obtained from Figure 3 as a upper limit for relaxation time;

Figure 11 displays the relationship between the modeled frequency shift of a 2 – 7 kHz linearly-swept chirp pulse, in Hz/ms, and the mean relaxation time of each sediment types listed in Table 1. The use of units of Hz/ms removes the effects of phase velocity on the equation used in

the modeling stage. This eliminates any errors that may be induced by inaccuracies in velocity, which will be particularly important for gassy sediments (Anderson and Hampton 1980). In addition the propagation of the pulse is modeled for all six sediment types listed in table 1 and allows the empirical relationship derived to be more tightly constrained than that obtained by LeBlanc *et al.* (1992).The relaxation time was calculated by applying a least squares linear fit to the region over which IF decreases with two-way time. The gradient of this line is then converted into a relaxation time using the empirical relationship derived from Figure 11, *i.e.*

$$\tau = 0.00672 f_{shift} .$$ (24)

where τ is relaxation time in μs and f_{shift} represents the gradient of the linear trendline applied in Hz/ms. This relaxation time can be used to calculate the attenuation using equation 12.
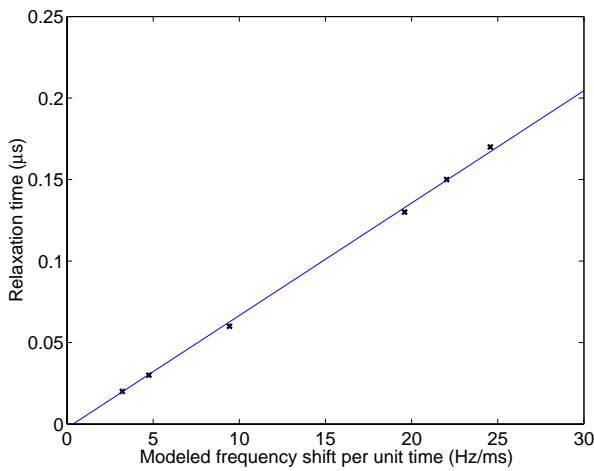

Figure 11: Plot of relaxation time against modeled frequency shift, in Hz/ms, for a 2-8 kHz linearly swept chirp pulse. Both modeled shift (X) and linear fit from which equation 25 is obtained (solid line) are displayed

As Figure 3 applies to saturated sediment, the third condition will be relaxed for IF results from Dibden Bay. Sediments here are gassy and will possess larger attenuations than saturated sediments. If the single relaxation time theory assumed is applicable to gassy sediments, this will result in larger relaxation times than expected.

The results of the techniques will be discussed in four stages. Firstly we will compare the use of uncorrelated and correlated data; secondly the best order of stacking will be examined; thirdly the optimum technique for estimating the IF of chirp data will be discussed; the fourth section will apply this optimum technique to the entirety of the two datasets used and discuss the resulting estimates of relaxation time and attenuation.

- **Comparison of correlated and uncorrelated data.**

Both datasets displayed similar results and typical results for an uncorrelated trace are included in Figure 12. The trace displayed is taken from a gassy region of the Dibden Bay dataset. The envelope of the uncorrelated trace is displayed in Figure 12(v), with the main signal event occurring between approximately 20 – 42 ms. The relatively broad and overlapping nature of reflection events, compared to those present in correlated data (Figure 13(v)) display the inability of uncorrelated data to locate reflection events accurately. Examination of the corresponding correlated trace, Figure 13(v), locates the peak of the seabed event at 14.6 ms, the peak of the gas horizon at 15.8 ms and the peak of the first multiple at 26 ms.

The IF estimated using the DCTF (Figure 12(i)) contains extremely large anomalies, with magnitudes greater than the Nyquist frequency of 12.5 kHz. However from 20 – 40 ms, *i.e.* over the duration of the main signal event, the majority of anomalies are less than 1 kHz and IFs which increase with two-way time, from 2.5 kHz at 20 ms to 4 kHz at 42 ms, can be observed. Estimations of IF arising from the STFT (Figure 12(i)) contain negligible anomalies. These are however replaced by discontinuities, with maximum magnitudes of 0.5 kHz for first moment estimates and 1.5 kHz for peak estimates. Decreasing trends in IF, which commence at two-way times corresponding to the seabed reflections, result in relaxation times greater than 1 µs. These are greater than expected, even for gassy sediments. Again IFs which increase with two-way time are observed over the duration of the main signal event. Estimates of IF derived from the WVD, (Figure 12(ii)) and PWVD (Figure 12(iii)), display similar general trends, with IF increasing with two-way time, over two-way times corresponding to the duration of the main signal and varying frequency ranges. Outside this region anomalies are relatively large and act to conceal any trends in IF. In general IF estimates arising from the first moment of TFDs display a region, which extends over the upper 5 ms of sediment, where IF decreases with two-way time. However the resulting relaxation times for this region are greater than 0.33 µs. Estimates of IF derived from the peaks of the XWVD (Figure 12(iv)) display IFs which generally increase with two-way time, while the location of IF trends arising from the first moment (Figure 12(iv)) display little correlation to the seabed location.

It is clear that techniques based on the first moment of TFDs produce the better IF estimations for uncorrelated data, than those based on the peak of TFDs. However little effective information about frequency shift and relaxation time can be obtained from uncorrelated data for the following reasons:

- The lack of temporal resolution of uncorrelated data;
- The poor signal to noise ratio of uncorrelated data;

- All IF estimations obtained from uncorrelated data are dominated by IFs that increase linearly with two-way time*, i.e.* we observe the increasing frequency of the emitted chirp pulse;

- Any regions where IF decreases with two-way time result in relaxation times greater than the expected upper limit;

- The use of sections of traces, as discussed in section 4.iv. simply reduced the amplitude of the anomalies present, with an IF which linearly increase with two-way time still dominating the results;

Figure 13 displays IF estimates for the *correlated* version of the trace discussed above and represent typical results for correlated data. The techniques used display similar characteristics to those previously observed, *i.e.* the DCTF estimates contain large anomalies, STFT estimates are disrupted by discontinuities and the smoothest IF estimates arise from the first moments of the WVD. However the important difference to IF estimates from uncorrelated data is the presence of IF trends, which decrease with two-way time and produce acceptable relaxation times.

Anomalies are generally smaller than those for uncorrelated data. This is a consequence of the increased signal to noise ratio achieved by correlation. The improved IF estimates are a consequence of two main factors. Firstly the duration of effective sampling pulse has been reduced from 4.5 ms to 0.15 ms. This allows reflection events to be more accurately resolved in time. Secondly the effective sampling pulse is now purely a broadband signal, *i.e.* it does not contain any linear chirp components. Hence IF now truly represents the central frequency of the signal. This assumption is of paramount importance if we wish to convert frequency shift per ms into useful geoacoustic parameters. Note that anomalous points still inhibit accurate estimation of both the gradient of the observed decreasing trends in IF and the two-way times at which such decreasing trends in IF commence. For some techniques anomalies completely conceal any trends in IF which may be present.

It is concluded that the use of correlated data produces IF estimates which are more applicable to the spectral shift technique of obtaining the geoacoustic properties of the sediment.
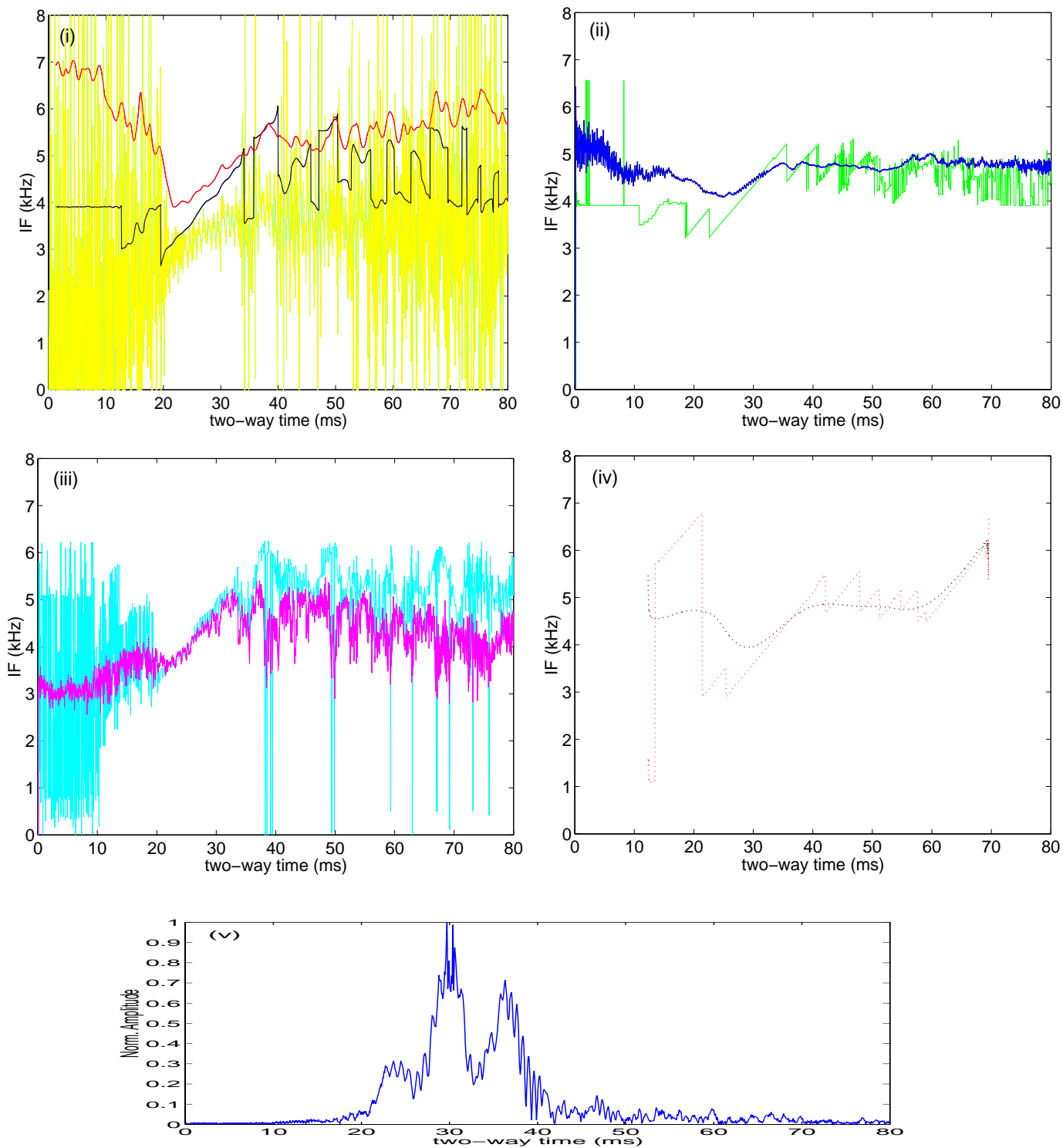
Figure 12: Typical results of IF techniques applied to a single uncorrelated trace, i.e. CDP 470 from Dibden Bay dataset.

(i)   IF estimate using DCTF (yellow), peak of STFT (black) and first moment of STFT (red).
(ii) IF estimate using peak (green) and first moment (blue) of WVD.
(iii) IF estimate using peak (cyan) and first moment (magenta) of PWVD.
(iv) IF estimate using peak (red dashed line) and first moment (black dashed line) of XWVD.
(v)   Envelope of uncorrelated trace used.
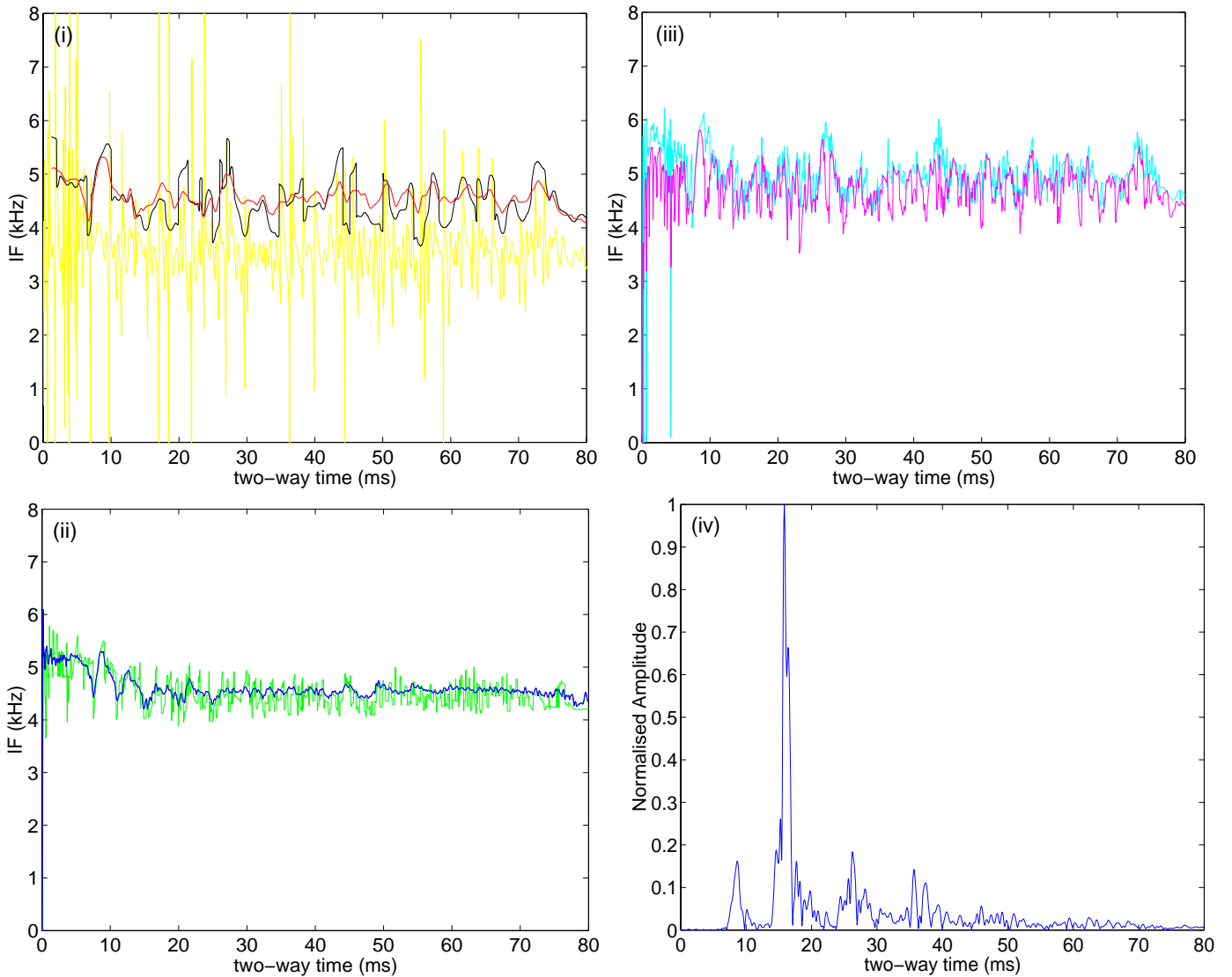
Figure 13: Typical results of IF techniques applied to a single correlated trace, i.e. CDP 470 from the Dibden Bay dataset.

(i)   IF estimate using DCTF (yellow), peaks of STFT (black) and first moment of STFT (red).
(ii)   IF estimate using peaks (green) and first moment (blue) of WVD.
(iii)   IF estimate using peaks (cyan) and first moment (magenta) of PWVD.
(iv)   Normalised envelope of correlated trace used.

- **Comparison of stacking orders.**

Figure 14 shows the application of the four stacking processes discussed in section 4.iv. to IF estimates obtained using the first moment of the WVD. The data displayed is for the section of correlated traces centred on CDP 470 from the Dibden Bay dataset.

The general features of the IF plot are displayed in Figure 14(i) and the envelope of the central trace displayed in Figure 14(ii). The IF decreases sharply with two-way time from 12.5 to 15 ms. This is followed by a sharper rise to a local peak at approximately 16 ms and then a linear decrease, which extends over approximately 5ms, at which point it rises sharply. This linear

40

decrease followed by sharp increase is repeated from 21 – 26 ms and 26 – 31 ms, with both the steepness of the linear decrease and the magnitude of the local peak in IF decreasing as the mean depth of the 5 ms section increases. The first and third local maxima, at approximately 16 ms and 26 ms, correspond well to peaks of the gas horizon and first multiple events respectively. Though the no such correspondence with any reflection event can be found for the second maximum, the repeatability of the trend suggests that it is the result of multiple reflections with a period of 5 ms.

It can be observed how the IF estimation resulting from the central trace of the section does not allow accurate observation of the afore mentioned trends. Estimations of IF that use the entire section display trends more clearly. The use of stacked IFs generates anomalies with the smallest magnitudes, i.e. less than 150 Hz. This allows trends in IF to most clearly observed, and so most accurately examined. The use of stacked traces typically generates anomalies with magnitudes up to 1 kHz, while the use of stacked distributions typically generates anomalies with magnitudes up to 500 Hz.
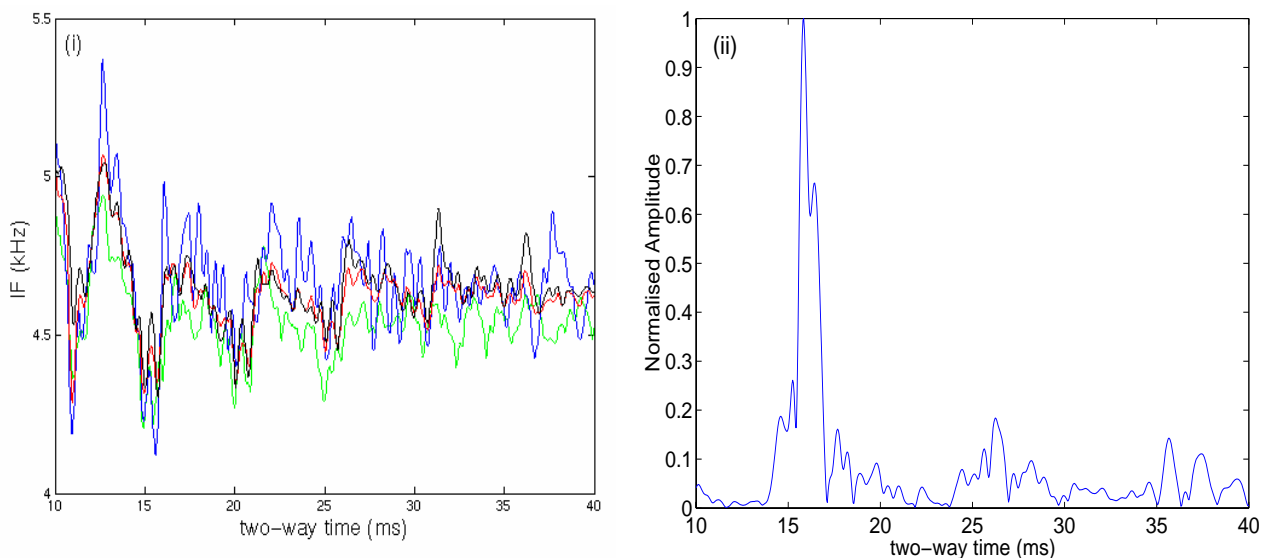

Figure14: Application of stacking to IF estimations, based on first moments of WVD, to section of 9 traces centred on CDP 479 form Dibden Bay dataset.
(i) IF estimations using; the central trace (green); stacked traces (blue), stacked IFs (red) and stacked distributions (black)
(ii) The normalized envelope of the central trace of the section.

The above conclusions are consistent across all techniques and sections examined with:

• IF estimates resulting from the central trace displaying trends that bear little relation to reflection events;

• IF estimates that use the entire section displaying trends that generally correspond to reflection events. The use of stacked IFs minimizes the magnitude of the anomalies, while

moderate anomalies are observed for stacked distributions and anomalies possess maximum magnitudes for the stacked traces approach;

These imply that the optimum manner of stacking is to estimate the IF of each trace in the section individually and stack the IF estimations to obtain a composite IF for the section.

- **C**omparison of selected techniques.

The techniques discussed in section 4.c.iv. were applied to the sections of correlated data, with the composite IF of the section calculated using the stacked IF approach. To maintain consistency Figure 15 displays results for the same section of traces from Dibden bay that has been used previously in this report. These results are typical for all other sections examined.

The IF estimates arising from the DCTF (Figure 15(i)) display lower IFs than expected, *i.e.* a mean IF of approximately 2.3 kHz. Anomalies possess typical magnitudes of 1 kHz. The fact that the composite IF of the section is less than the IF of the single central trace, *i.e.* the yellow line in Figure 13(i), implies that stacking does not enhance DCTF estimations of IF. This is probably a result of the large anomalies that dominate DCTF estimates.

Figures 15(ii) to 15(iv) display how first moment estimates of IF possess anomalies with magnitudes typically less than 50% of those present in the corresponding peak estimations. Hence first moment estimates produce smoother IFs. These provide a more accurate basis for the estimation of frequency shift, relaxation time and other geoacoustic parameters.

The IF estimates obtained from the moments of the STFT (Figure 15(ii)) possess negligible anomalies. However IF trends observed generally exhibit poor correlation to the observed reflection events.

Estimates of IF derived from first moments of the WVD (Figure 15(iii)) display IF ranging from 4.1 - 4.7 kHz in the sediment. Owing to the preferential attenuation of higher frequencies, the central frequency of the received pulse is expected to be lower than 4.5 kHz*, i.e.* the central frequency of the emitted pulse. Hence the range of IF values obtained by this technique appear reasonable, with high-frequency noise possibly being the source of IF values greater than 4.5 kHz. Anomalies are typically less than 100 Hz and IF displays a smooth variation with two-way time. The events and trends observed in IF, such as the sharp rise in IF followed by a region over which IF decreases linearly with two-way time mentioned earlier, correlate well to observed reflection events. In addition relaxation times, resulting from the application of first-order least squares fits to regions where IF decreases with two-way time, typically lie within the acceptable limits of $0 - 0.2$ μs. However, for all sections analysed, IF estimations which use the WVD display a region of two-way times, which commences between 41 ms and 43 ms and possess a duration of $5 - 7.5$ ms, where IF

decreases with two-way time. As other techniques display "hints" of this trend and a reduction in the data length examined did not change the location of this trend it is concluded that this represents a real event which is present in the correlated data and not an artifact of the IF estimation technique used. However this event may be a consequence of the acquisition or correlation of the data and may not represent a geological horizon.
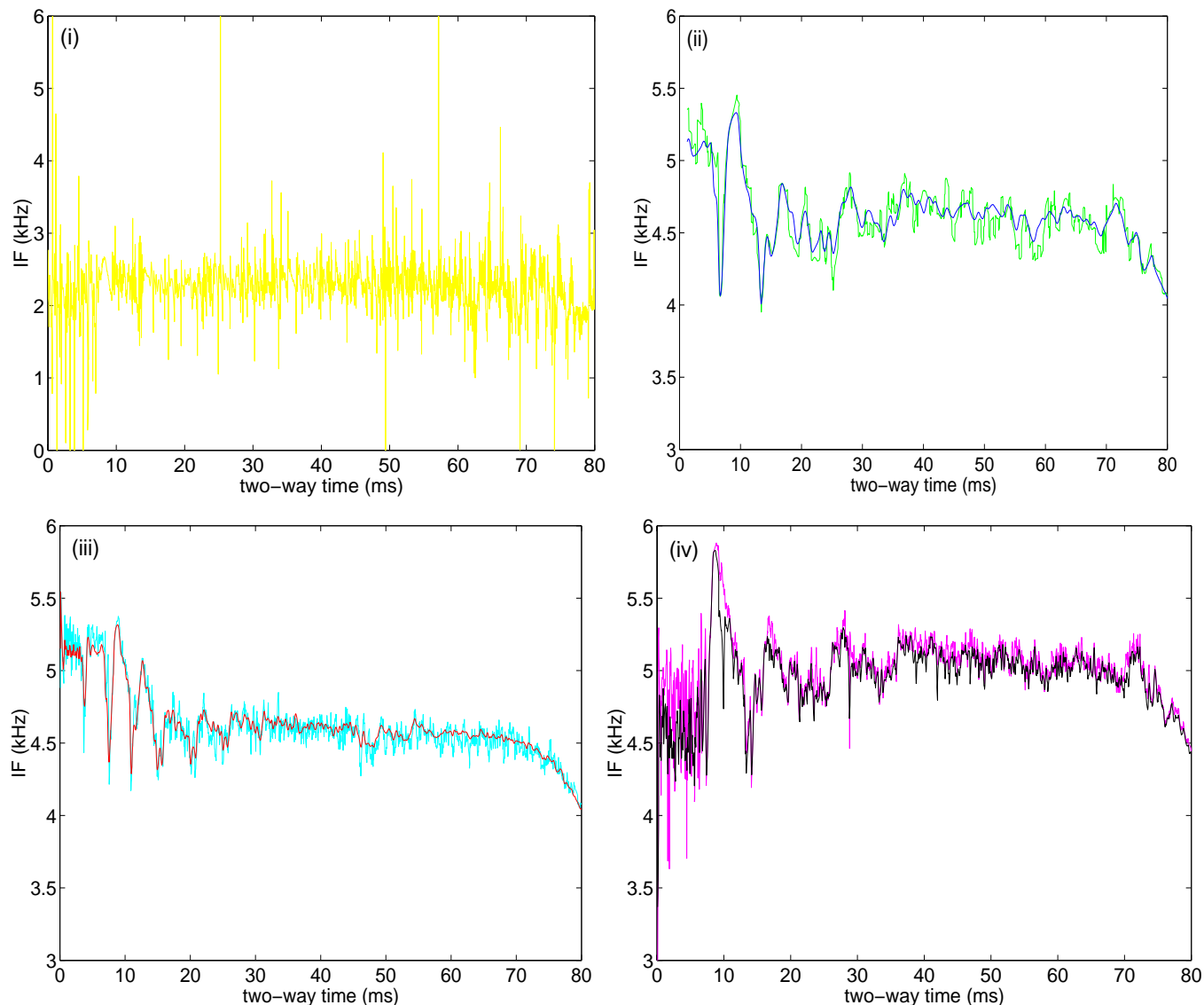

Figure 15: Comparison of seven IF estimation techniques applied to sections of correlated data. Composite IF is obtained using stacked IF approach.
(i)   IF estimations from DCTF (yellow).
(ii)   IF estimations from peaks (green) and first moments (blue) of STFT.
(iii)   IF estimations from peaks (cyan) and first moments (red) of WVD.
(iv)   IF estimations from peaks (magenta) and first moments (black) of PWVD.
Data used is section of 9 traces centred on CDP 470 of the Dibden Bay dataset.

IF estimates constructed from the moments of the PWVD (Figure 15(iv)) also display events and trends that correspond well to observed reflection events. Resulting estimates of relaxation time are generally within accepted limits and anomalies typically less than 200 Hz in the sediment.

However, the majority of IF values are greater than 5 kHz, which is greater than the expected values of 4.5 kHz or lower. This raises doubt in IF estimates produced by this technique.

For all IF estimation techniques, particularly those that use TFDs, the IF appears to drop off over the last 20 ms of the trace. It is hypothesized that, beyond 60 ms, the SNR of the signal drops below the level at which IF can be accurately estimated. The high level of noise in IF estimates below this point result in ineffective stacking.

As we are primarily interested in the uppermost sediments, where SNR is highest, using the first moment of the WVD appears to be the optimum IF estimation technique. This produces:

- IF which vary smoothly with two-way time and possess anomalies with magnitudes typically less than 100 Hz;
- IF values approximately that expected;
- Events and trends in IF that correspond well to observed reflection events;
- Estimates of relaxation time which generally lie within accepted limits;

However the presence of a possible artifact centred on approximately 45 ms and an IF that decreases over the last 20 ms of analysed data limits the use of this techniques to the upper 40ms of correlated data.

- **Application of optimum technique.**

The IF estimation technique that performed best in these trials, *i.e.* the estimation of IF using the first moment of the WVD and the stacking of IF across a nine trace section of correlated data, was used to estimate the relaxation time and attenuation of chirp data, as described earlier in section 4.v. In the case of the dataset from Dibden Bay it was difficult to locate a peak in the seabed reflection, as this event merged with the stronger reflection from the gas horizon. IF appears to decrease in a linear fashion with two-way time from two-way times that correspond to peaks in gas horizon reflection events to those that correspond to peaks in the first multiple of the gas horizon. Hence the least-squares linear fit is applied between these two limits. Typical results are displayed in Figure 15, for the same section from Dibden Bay used previously. The linear plot results in a relaxation time of 0.01 μs and an attenuation of 0.02 dB/m for the central frequency of the emitted pulse, i.e. 4.5 kHz, and predicted velocity of 1500 m/s. These are clearly incorrect for gassy sediments, which possess large attenuations of the order of 100 dB/m, and may arise for a range of reasons. Firstly the linear line incorporates two distinct events and does not truly represent the variation of IF with two-way time. However as no reflection event corresponds to the two-way time at which the second event commences, one cannot justify the use of a linear fit which incorporates the first event only, the use of which would result in much higher relaxation times and attenuations.

Secondly the fundamental equation, equation 12, which is used to obtain relaxation time from frequency and convert relaxation time into attenuation assumes a quadratic relationship between attenuation an frequency. This is not applicable to gassy sediments were the attenuation depends on the resonant frequency of the gas bubbles present (Anderson and Hampton 1980). In addition the velocity assumed above may also be significantly in error.
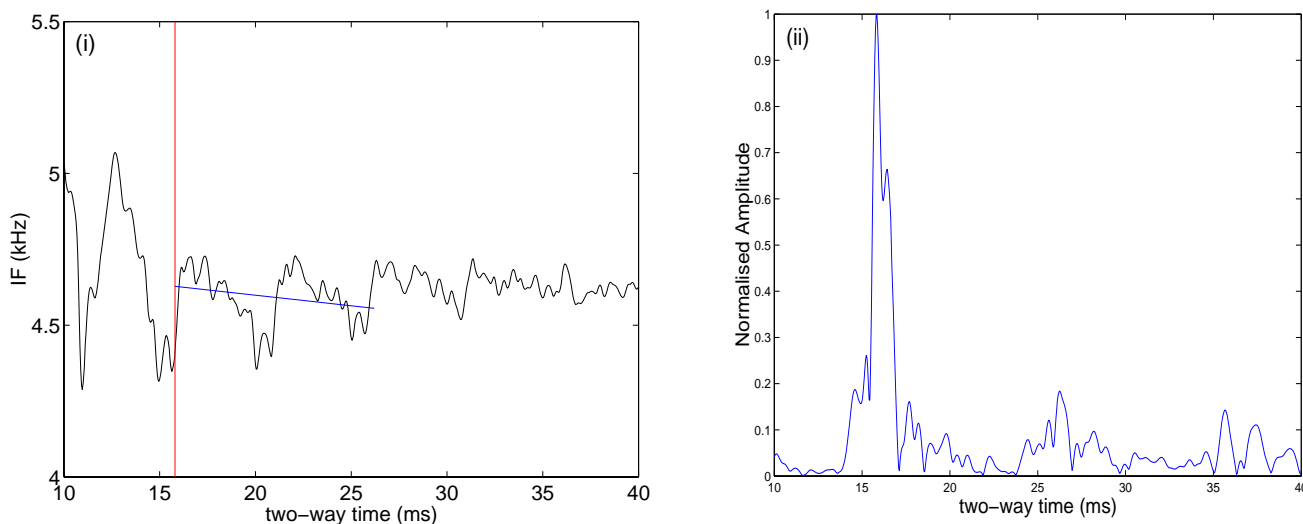

Figure 16: Results of optimum IF estimation techniques applied to data from Dibden dataset.
(i)   IF estimation, with two-way time of gas horizon peak (red line) and trendline from two-way time of gas horizon peak to two-way time of peak in first multiple of gas horizon (blue line).
(ii) Normalised amplidue of central trace
Data is section of 9 traces centred on CDP 470.

However, when applied to the Bouldnor Cliff dataset, results proved more promising. The clearly resolved nature of the seabed reflections allow the least-squares fit to be selected with greater confidence. The application of a least-squares fit is displayed in Figure 17. This fits the data much better than in Figure 16 and results in a relaxation time of 0.1 µs and an attenuation of 0.2 dB/m.

Figure 18 results from the application of such least-squares fits to the first 700 CDPs of the Bouldnor Cliff dataset. The rest of this dataset was neglected as the peaks of the first multiple event could not be accurately located. The resulting frequency shifts (Figure 18(i)) all display negative values. Corresponding relaxation times (Figure 18(ii)) all lie below 0.14 µs, which are within accepted limits. Resulting attenuations at 4.5 kHz are all less than 0.32 dB/m. These result in Q values greater than 30, which appear reasonable for the saturated sediments and sedimentary rocks under examination. There is however a large degree of variation from one section to the next. Assuming that sediments display small lateral variations, resulting estimates of relaxation time and attenuation should vary smoothly with central CDP. This scatter is particularly noticeable for sections with central CDPs greater than 525, the reason for this unknown.
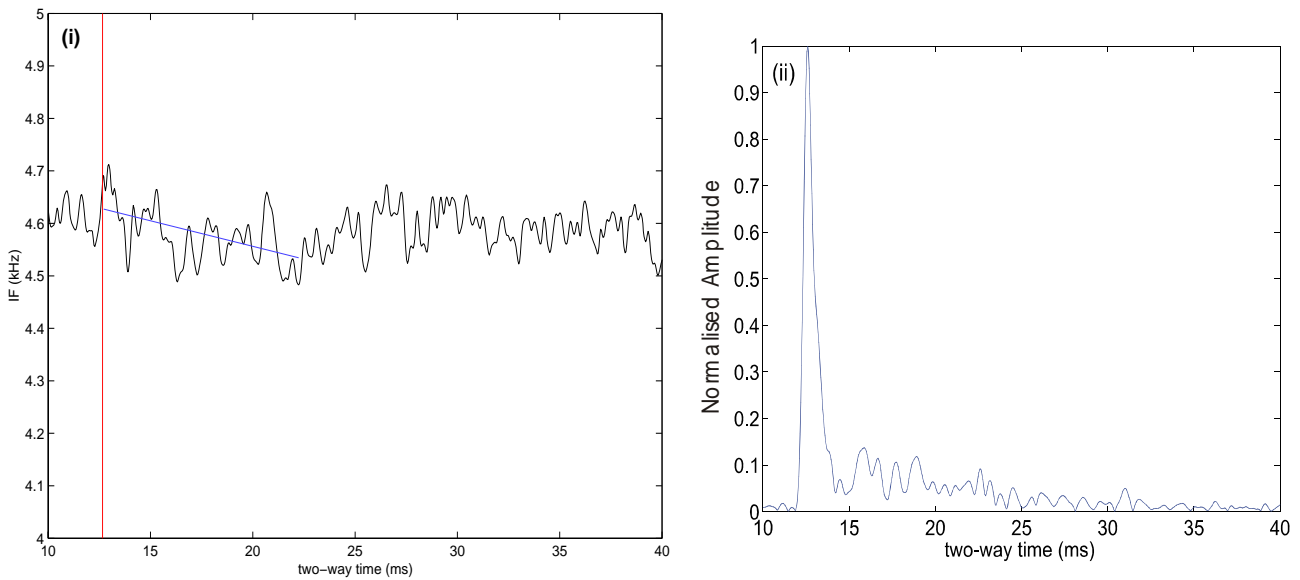
Figure 17: Application of optimum IF estimation technique to data from Bouldnor Cliff dataset.
(i) IF estimation, with location of seabed peak (red line) and trendline from seabed to first multiple (blue line) marked.
(ii) Normalised amplitude of central trace, displaying seabed and sub-surface reflections.
Data used is section of 9 traces centred on CDP 25.
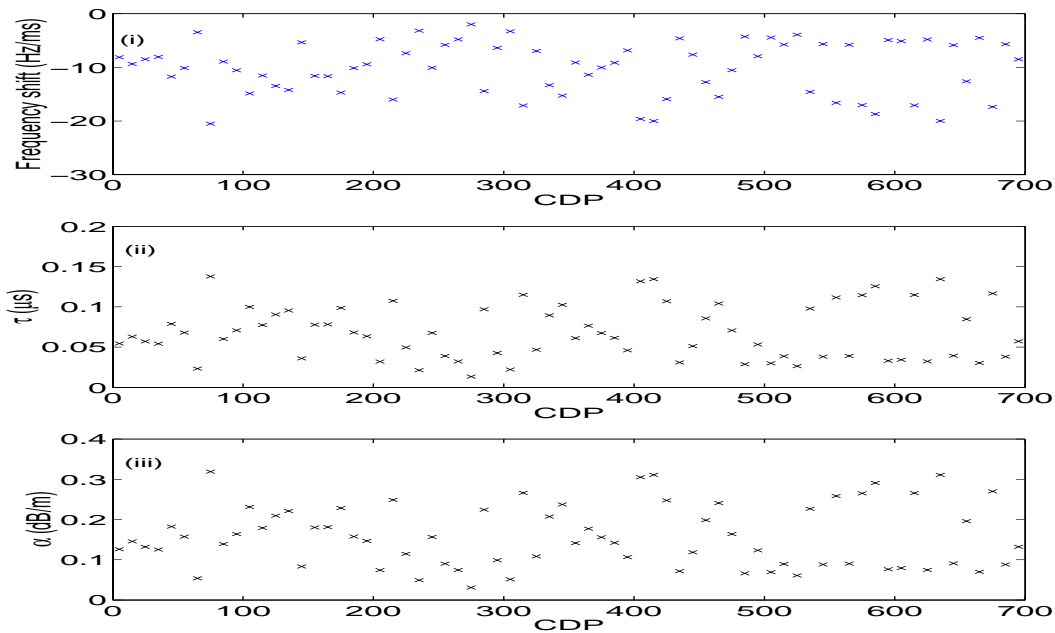
Figure 18: Estimation of: (i) Frequency shift; (ii) Relaxation time; (iii) Attenuation at 4.5 kHz
For first 700 CDPs from Bouldnor Cliff Dataset.

IVf   Conclusions.

Work to date has dealt with the development of a technique that can accurately estimate the IF of chirp reflection data. This has been achieved with the technique outlined below:

- Divide the *correlated* chirp profile into a series of sections, each containing a fixed number of adjacent traces;

- In each section estimate the IF of each trace using the first moment of the WVD;

- Stack the resulting IF to obtain a composite IF for the section;

IF estimates obtained from this technique are only valid for the upper 40 ms of received data, with estimates below this becoming less realistic. A section size of 9 traces was selected in this report. Estimates of geoacoustic parameters obtained using least-square linear fits to IF above the first multiple, and the approach outlined by LeBlanc *et al.* (LeBlanc, Panda et al. 1992) appear realistic in the case of saturated sediments, *i.e.* the Bouldnor Cliff dataset. However in the case of gassy sediments, *i.e.* the Dibden Bay dataset, estimated attenuations are dramatically lower than expected. Concern is raised about whether the intrinsic equation used, equation 12, in both the conversion of shift in central frequency to relaxation time and the calculation of attenuation is applicable to marine sediments. Previous research suggests that the quadratic relationship between attenuation and frequency is valid for neither saturated nor gassy sediments.

Hence the aims of future work are:

- To develop a reliable method of converting shift in central frequency into geoacoustic parameters, e.g. for saturated sediments use an attenuation α_{dB} that varies linearly with frequency f (Hamilton 1972; Hamilton 1979; Toksoz, Johnstone et al. 1979):

$$\alpha_{dB} = kf \tag{25}$$

where k is a parameter that depends on sediment properties, such as grain size and porosity. The shift per unit time in the central frequency of the emitted chirp pulse could then be modelled for a range of k and so sediment types. If the velocity of the sediment layers present could be obtained, the theoretical relationship between frequency shift and k could be used to invert measured shifts in central frequency into values of k and α_{dB}. Note that the use of an attenuation linearly related to frequency requires knowledge of the velocity, while the quadratic relationship used previously, (LeBlanc, Panda et al. 1992), does not require this information.

In theory a model which incorporates the frequency dependent attenuation displayed by gassy sediments could be used for such environments, though the more complex nature of this relationship may make this process problematic;

- To assess the smallest window in two-way time over which the optimum technique selected can be used to reliable estimate shift in central frequency. This will dictate the minimum thickness of sediment layers that can be resolved. Previous work on IF has neglected the issue of windowing by simply applying linear fits to IF values between the seabed and first multiple reflections. However this may contain a variety of sediment layers and will hence produce a

composite attenuation for all sediment layers present. The introduction of smaller windows of two-way time will may allow these layers be both resolved and examined individually.

References.

Anderson, A. L. and L. D. Hampton (1980). "Acoustics of gas bearing sediments 2. Measurements and models." <u>Journal of the Acoustical Society of America</u> **67**(6): 1890-1905.

Anderson, A. L. and L. D. Hampton (1980). "Acoustics of gas bearing sediments 1. Background." <u>Journal of the Acoustical Society of America</u> **67**(6): 1865-1889.

Barkat, B. and B. Boashash (1999). "Instantaneous Frequency Estimation of Polynominal FM Signals Using the Peak of the PWVD: Statisical Performance in the Presence of Additive Noise." <u>IEEE Transactions on Signal Processing</u> **47**(9): 2480-2491.

Best, A. I., Q. J. Higgett, et al. (2001). "Comparison of in-situ and acoustic measurements on Lough Hyne marine sediments." <u>Journal of the Acoustical Society of America</u> **100**(2): 695-709.

Boashash, B. (1988). "Note on the Use of the Wigner Distribution for Time-Frequency Signal Analysis." <u>IEEE Transactions on Acoustics, Speech and Signal Processing</u> **36**(9): 1518-1521.

Boashash, B. (1992). "Estimating and Interpreting The Instantaneous Frequency of a signal-Part 1: Fundamentals." <u>Proceedings to the IEEE</u> **80**(4): 520-538.

Boashash, B. (1992). "Estimating and Interpreting The Instantaneous Frequency of a Signal-Part 2: Algoritms and Applications." <u>Proceedings to the IEEE</u> **80**(4): 539-568.

Boashash, B. and P. O'Shea (1993). "Use of the Cross Wigner-Ville Distribution for Estimation of Instantaneous Frequency." <u>IEEE Transactions on Signal Processing</u> **41**(3): 1439-1445.

Boashash, B. and P. O'Shea (1994). "Polynominal Wigner-Ville Distributions and Their Relationship to Time-Varying Higher Order Spectra." <u>IEEE Transactions on Signal Processing</u> **42**(1): 216-220.

Bowles, F. A. (1997). "Observations on attenuations and shear wave velocity in fine-grained, marine sediments." <u>Journal of the Acoustic Society of America</u> **101**(6): 3385-3397.

Buckingham, M. J. (2000). "Wave propagation, stress relaxation, and grain-to-grain shearing in saturated, unconsolidated marine sediments." <u>Journal of the Acoustic Society of America</u> **108**(6): 2798-2815.

Cohen, L. (1995). <u>Time-Frequency analysis.</u>, Prentice-Hall Inc.: 299.pp

Courtney, R. C. and L. A. Mayer (1993). "Calculation of acoustic parameters by a filter-correlation method." <u>Journal of the Acoustical Society of America</u> **93**(2): 1145-1154.

Dasios, D., T. R. Astin, et al. (2001). "Compressional-wave Q estimation from full-waveform sonic data." <u>Geophysical Prospecting</u> **49**: 353-373.

Dix, J. K., N. Jarvis, et al. (2000). <u>A reconstruction of the paleolandscape of Bouldnor Cliff, Isle of Wight.</u> 33rd Conference on Historical Archeology: Waterways and Landscapes., Quebec city, Canada, Society of Historical Archeology.

Hamilton, E. L. (1972). "Compressional-wave attenuation in marine sediments." <u>Geophysics</u> **37**(4): 620-646.

Hamilton, E. L. (1979). "Sound velocity gradients in marine sediments." <u>Journal of the Acoustical Society of America</u> **65**(4): 909-922.

Hamilton, E. L. (1979). "Vp/Vs and Poisson's ratio in marine sediments and rocks." <u>Journal of the Acoustical Society of America</u> **66**(4): 1093-1101.

Hamilton, E. L. (1987). Acoustic properties of sediments. <u>Acoustics and ocean bottom</u>. A. lara-Saenz, C. Ranz-Guerra and C. Carbo-Fite**:** 279.

Jannsen, D., J. Voss, et al. (1985). "Comparison of methods to determine Q in shallow marine sediments from vertical reflection seismograms." Geophysical Prospecting **33**: 479-497.

Johnstone, D. H. and M. N. Toksoz (1981). Definitions and terminology. Seismic wave attenuation. M. N. Toksoz and D. H. Johnstone, Society of Exploration Geophysics**:** 1-5.

Kearey, P. and M. Brooks (1991). An introduction to geophysical exploration, Blackwell Science: 254.pp

LeBlanc, L. R., L. Mayer, et al. (1992). "Marine sediment classification using the chirp sonar." Journal of the Acoustical Society of America **91**(1): 107-115.

LeBlanc, L. R., S. Panda, et al. (1992). "Sonar attenuation modeling for classification of marine sediments." Journal of the Acoustical Society of America **91**(1): 116-126.

Maroni, C. S. and A. Quinquis (1997). Estimation of chirp sonar signal attenuation for classification of marine sediments: Improved Spectral ratio method. High frequency acoustics in shallow water, Lerici, Italy:347-354.

Marple, S. R. (1999). "Computing the Discrete-Time "Analytic" Signal via FFT." IEEE Transactions on Signal Processing **47**(9): 2600-2603.

Matheney, M. P. and R. L. Nowack (1995). "Seismic attenuation values obtained from instantaneous-frequency matching and spectral ratios." Geophysics Journal International **123**: 1-15.

McCann, C., J. Sothcott, et al. (1998). Low frequency measurements of the acoustic properties of seafloor sediments under confining pressures to 3.5 MPa. Oceanology International 98-The Global Ocean, Brighton, UK:10-13.

Panda, S., L. R. LeBlanc, et al. (1994). "Sediment classification based on impedance and attenuation estimation." Journal of the Acoustical Society of America **96**(5): 3022-3035.

Quinn, R., Ed. (1997). Marine high-resolution seismology: Acquisition processing and applications. School of Ocean and Earth Science. Southampton, Southampton.

Quinn, R., J. M. Bull, et al. (1998). "Optimal processing of Marine High Resolution Seismic Reflection (Chirp) Data." Marine Geophysical Researches **20**: 13-20.

Richardson, M. D. and K. B. Briggs (1993). "On the use of acoustic impedance values to determine sediment properties." Proceedings to the Institute of Acoustics **15**(2): 15-23.

Ristic, B. and B. Boashash (1996). "Instantaneous Frequency Estimation of Quadratic and Cubic FM Signals Using the Cross Polynominal Wigner-Ville Distribution." IEEE Transactions on Signal Processing **44**(6): 1548-1553.

Robb, G. B. O. (2000). A multitechnical analysis of the shallow gas blanket in Southampton Water. School of Ocean and Earth Science. Southampton, Southampton**:** 52.pp

Sheriff, R. E. and L. P. Geldart (1995). Exploration Seismology, Cambridge Unieversity Press: 592.pp

Sills, G. C., S. J. Wheller, et al. (1991). "Behaviour of offshore soils containing gas bubbles." Geotechnique **41**: 227-241.

Stoll, R. D. (2002). "Velocity-dispersion in water saturated granular sediment." Journal of the Acoustical Society of America **111**(2): 785-793.

Taner, M. T., F. Koehler, et al. (1979). "Complex seismic trace analysis." Geophysics **44**(6): 1041-1063.

Tarif, P. and T. Bourbie (1987). "Experimental comparison between spectral ratio and rise time techniques for attenuation measurements." Geophysical Prospecting **35**: 668-680.

Toksoz, M. N., D. H. Johnstone, et al. (1979). "Attenuation of seismic waves in dry and saturated rocks: 1. Laboratory measurements." Geophysics **44**(4): 681-690.

Tuffin, M. (1997). The reflection characteristics of shallow gas formations. School of Ocean and Earth Science. Southampton, Southampton**:** 55.pp

Tuffin, M. (2001). The geoacoustic properties of shallow gas bearing sediments. <u>School of Ocean and Earth Science</u>. Southampton, Southampton**:** 149.pp